Polymers

18.S995 - L12 & 13

dunkel@mit.edu

DNA = biopolymer pair

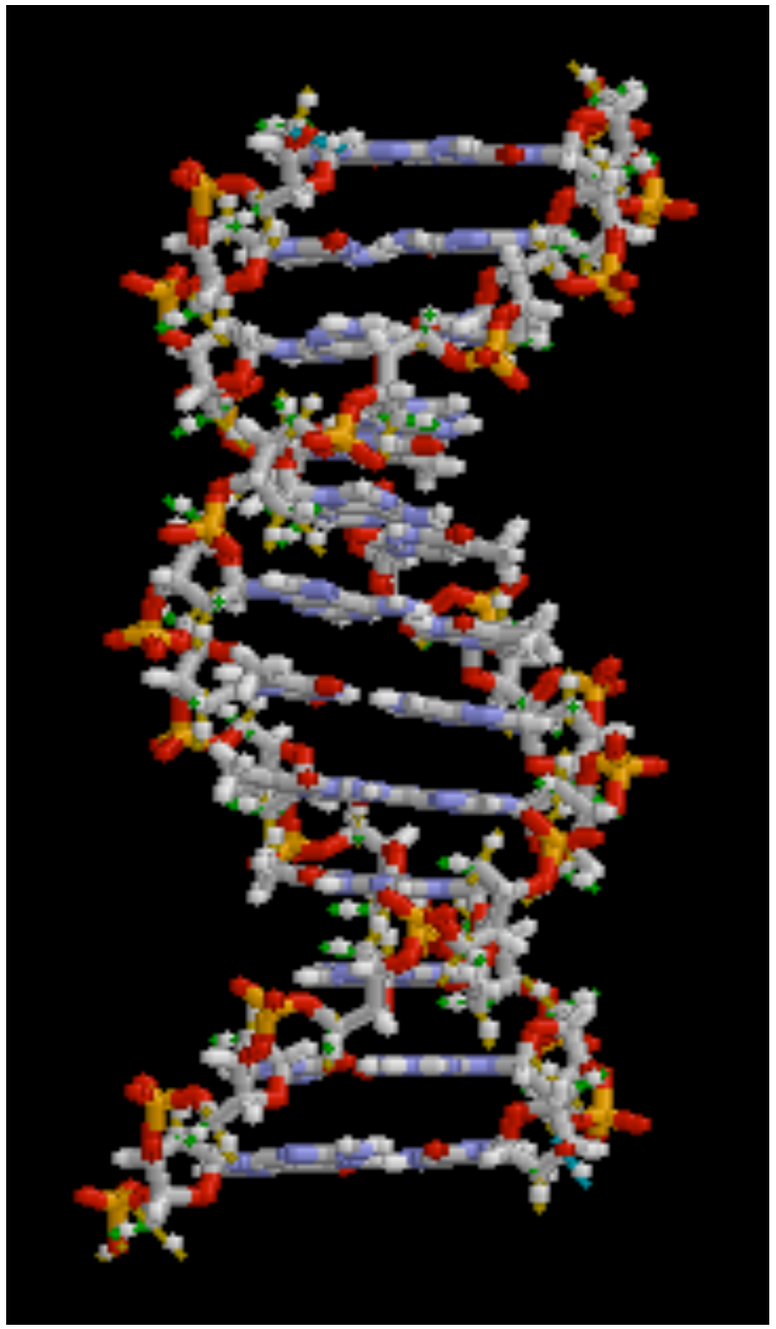

~ 3m per cell

~ 10^14 cells/human

> max. distance between Earth and Pluto
(~50 AU = 7.5 x 10^12 m)

dunkel@math.mit.edu

DNA packaging

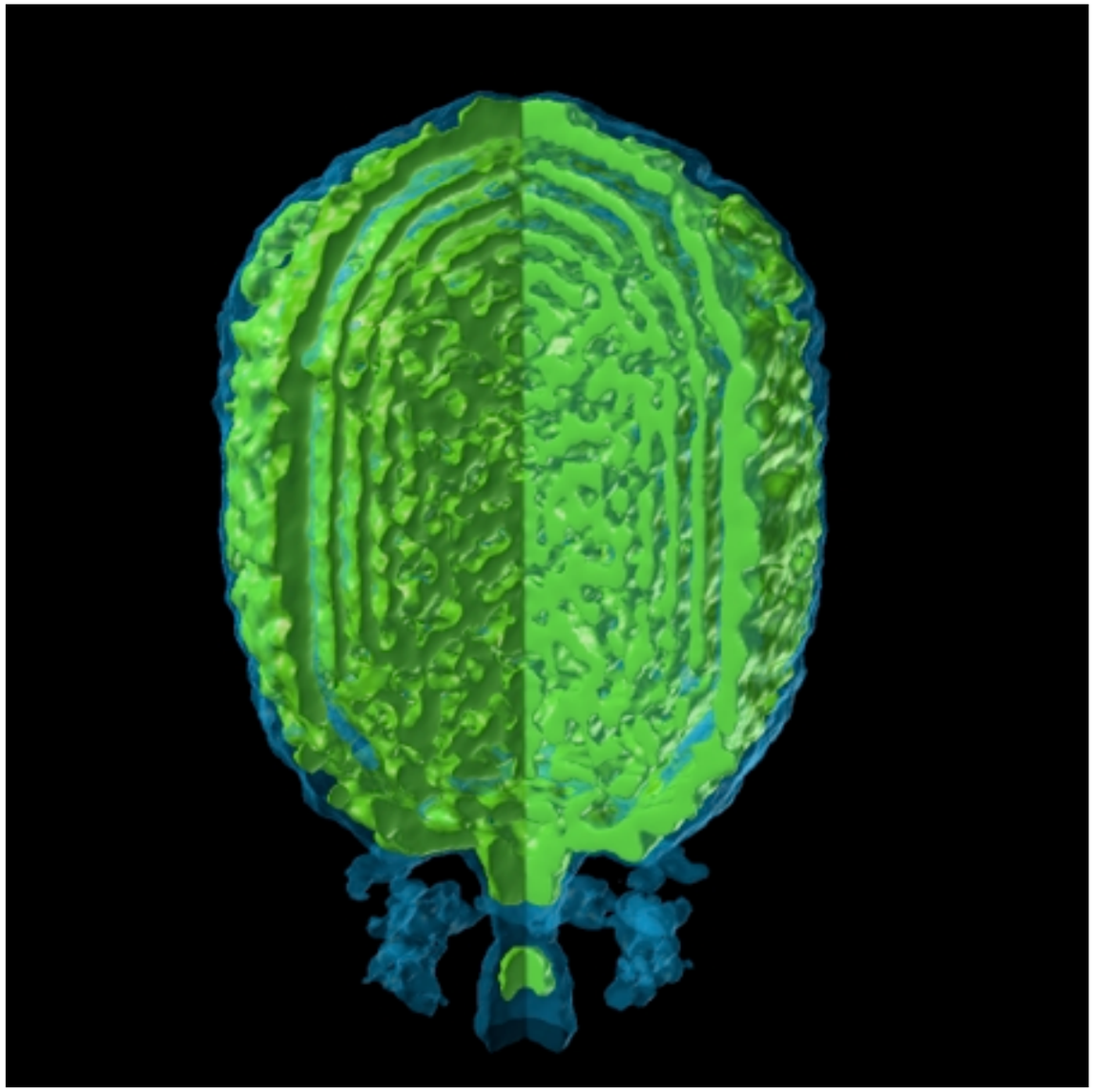

Virus Phi-29

http://www.mit.edu/~kardar/teaching/projects/dna_packing_website/

dunkel@math.mit.edu

DNA packaging in eukaryotes

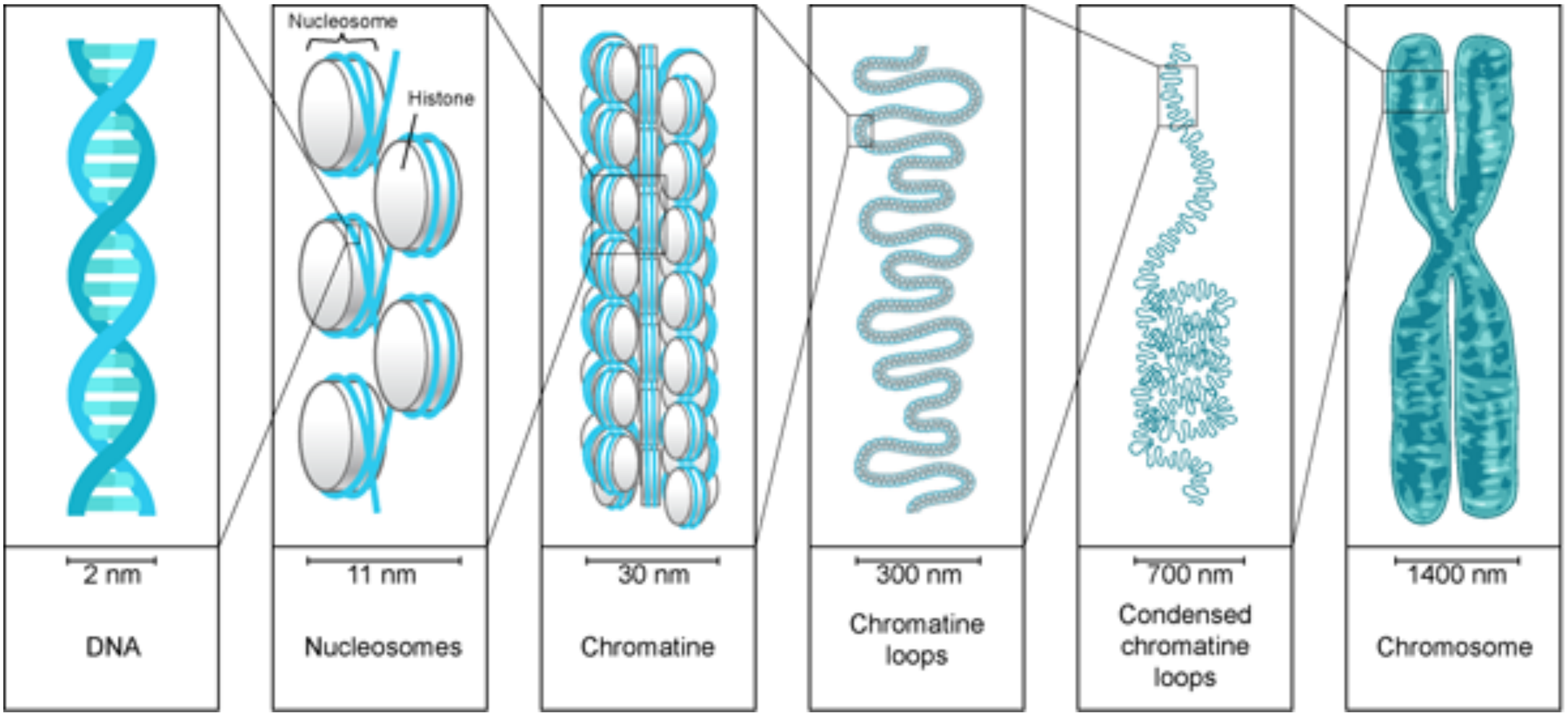

dunkel@math.mit.edu

Nucleosomes

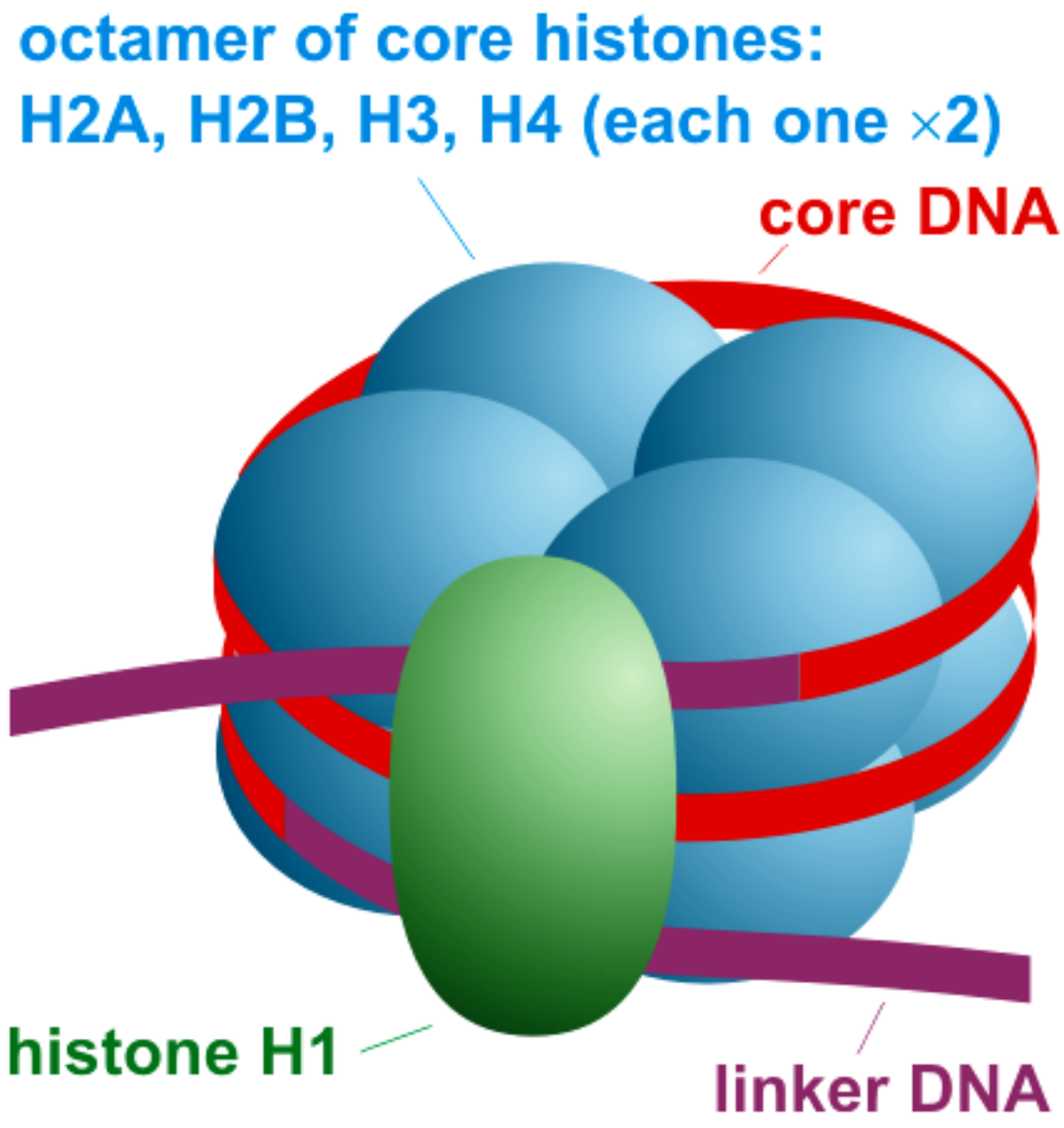

dunkel@math.mit.edu

DNA packaging in eukaryotes

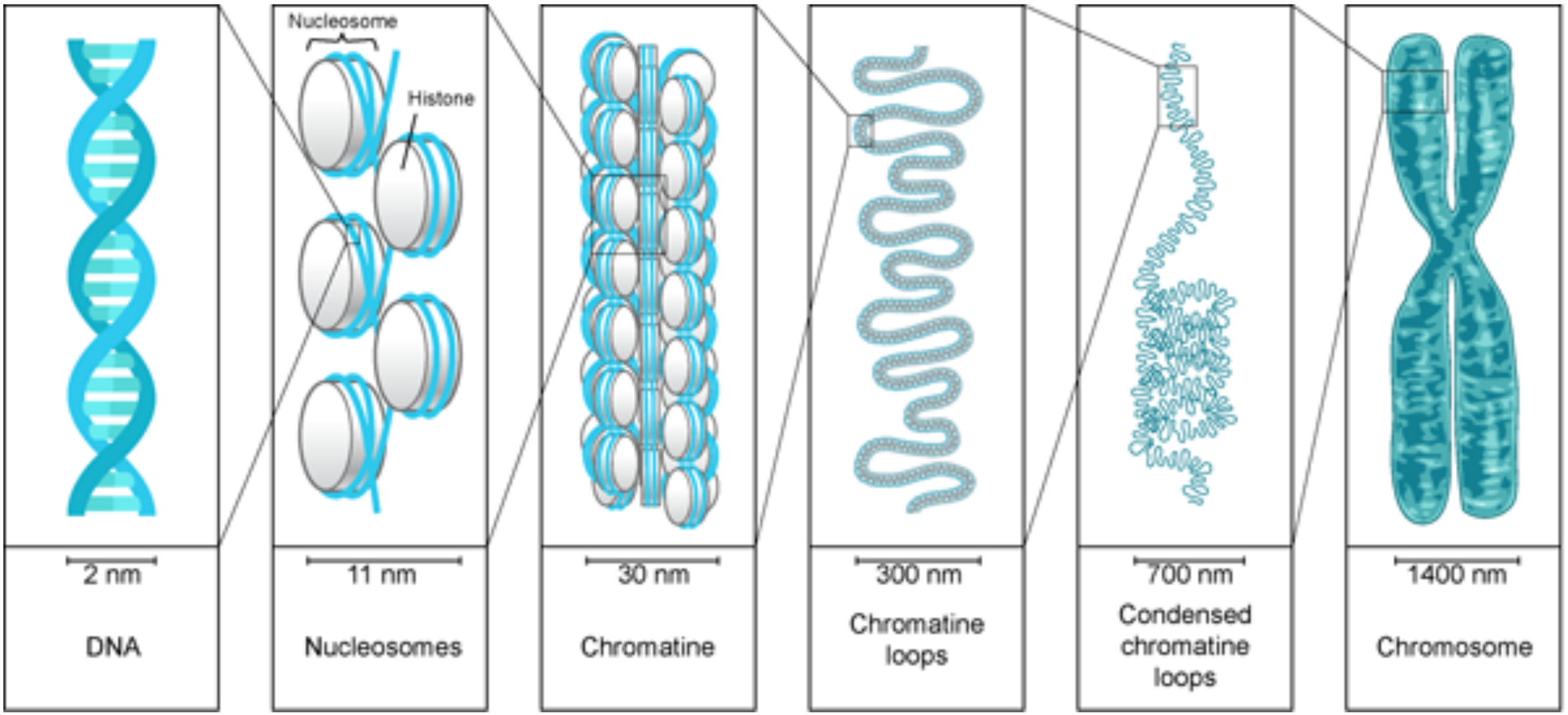

dunkel@math.mit.edu

DNA packaging in humans

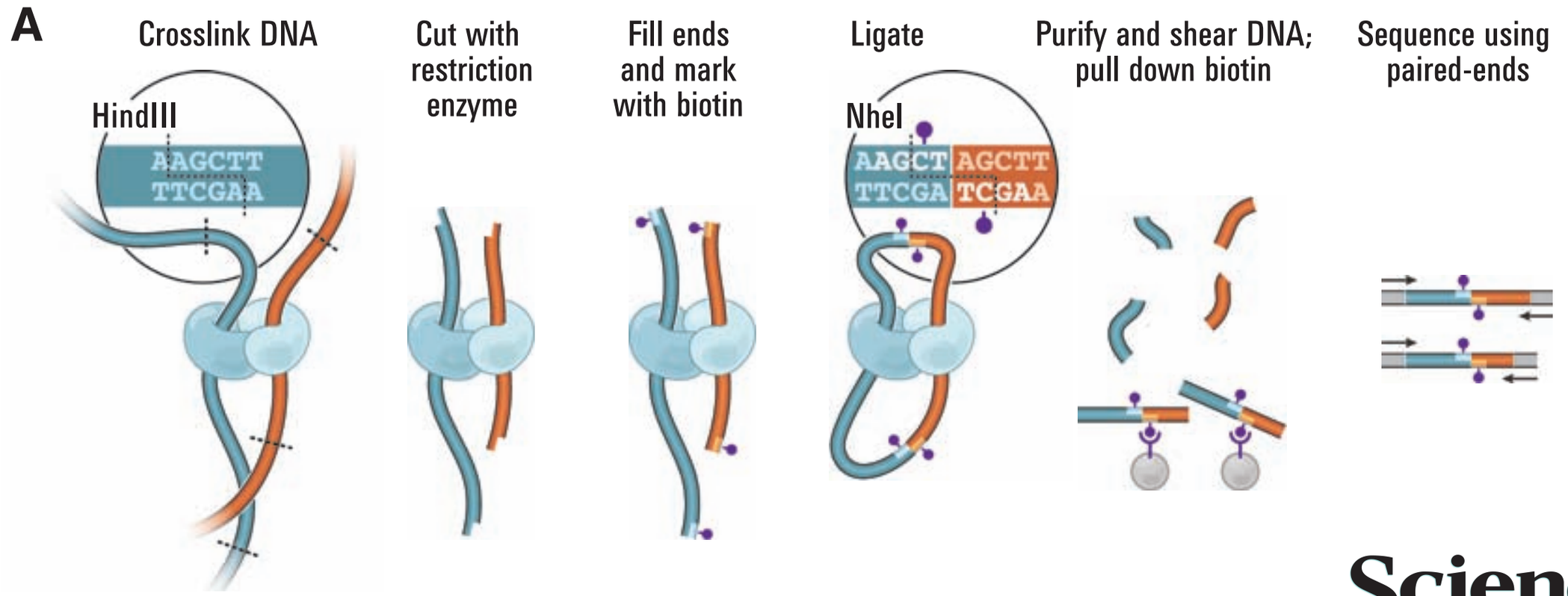

Lieberman-Aiden et al. (2011) Science

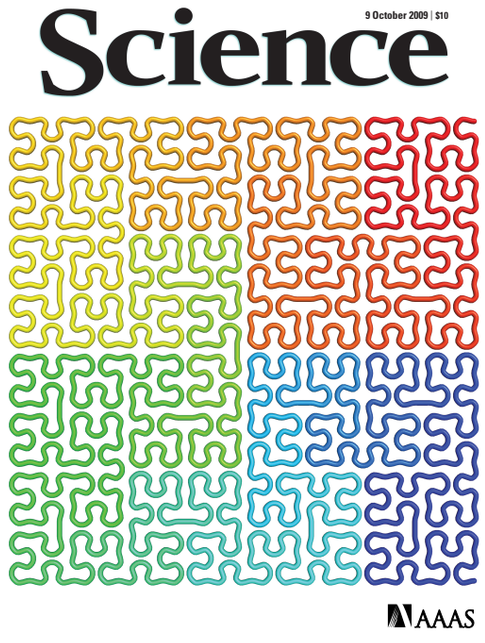

dunkel@math.mit.edu

DNA packaging in humans

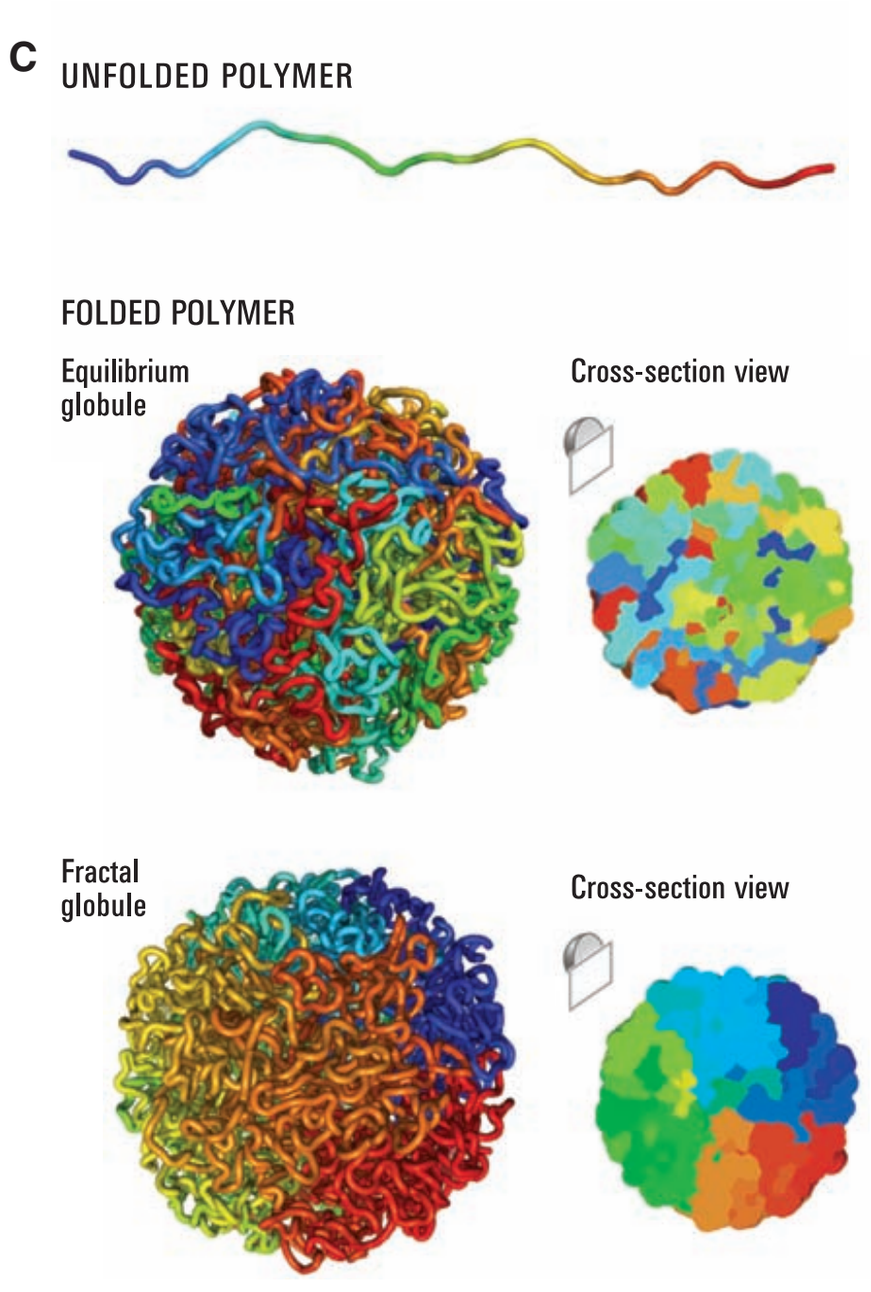

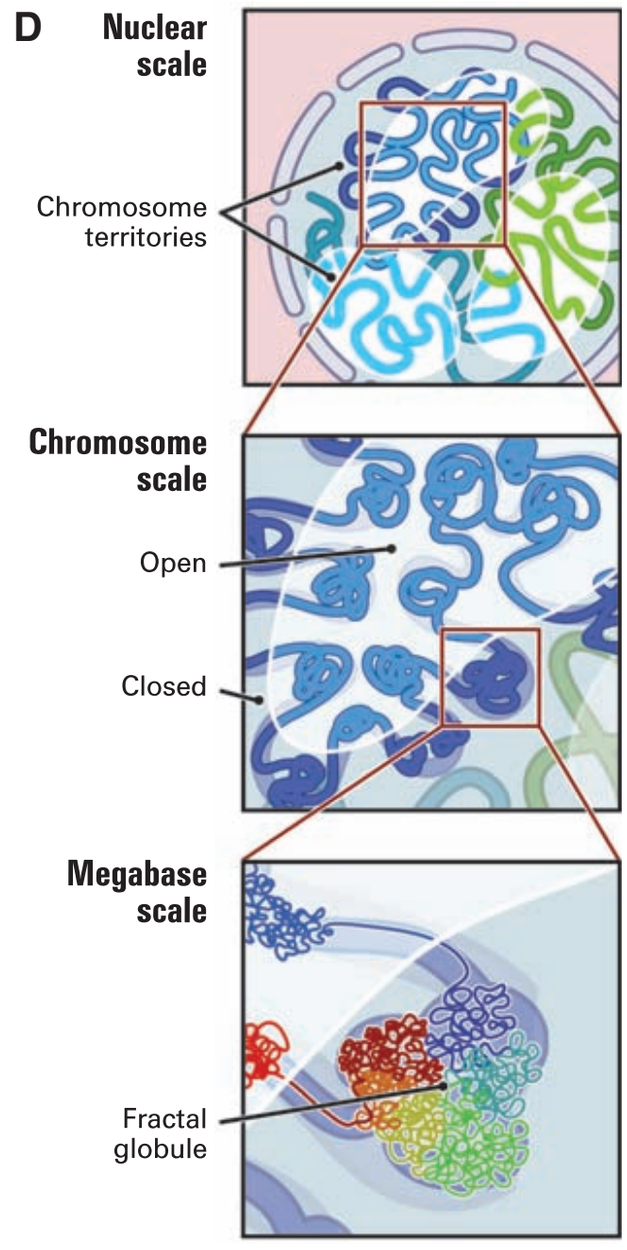

Lieberman-Aiden et al. (2011) Science

dunkel@math.mit.edu

Cyto-skeleton

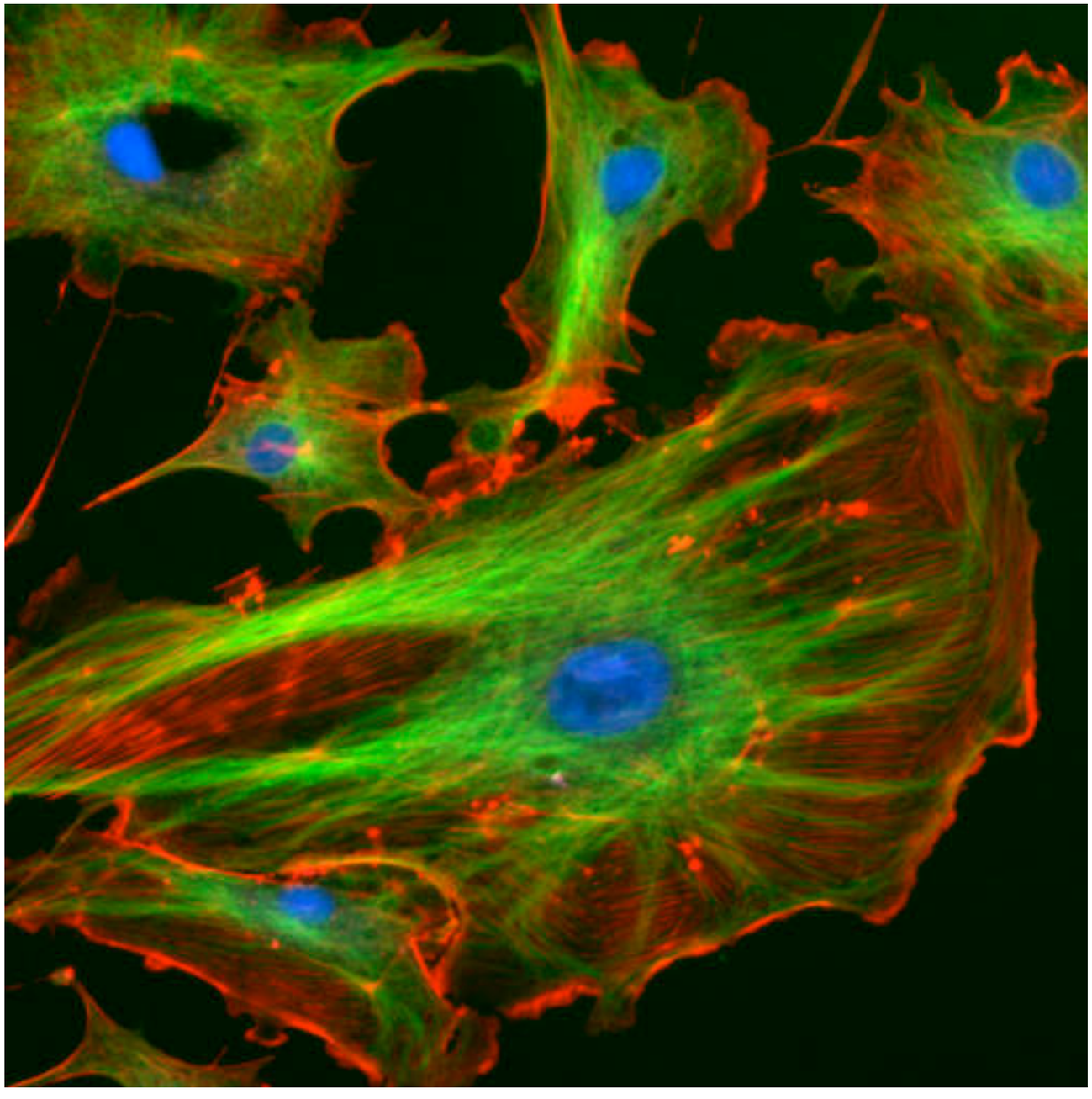

Nucleus

Actin

Microtubuli

mechanical properties,
network topology, ...

eukaryotic cells (source: wiki)

dunkel@math.mit.edu

Cyto-skeleton

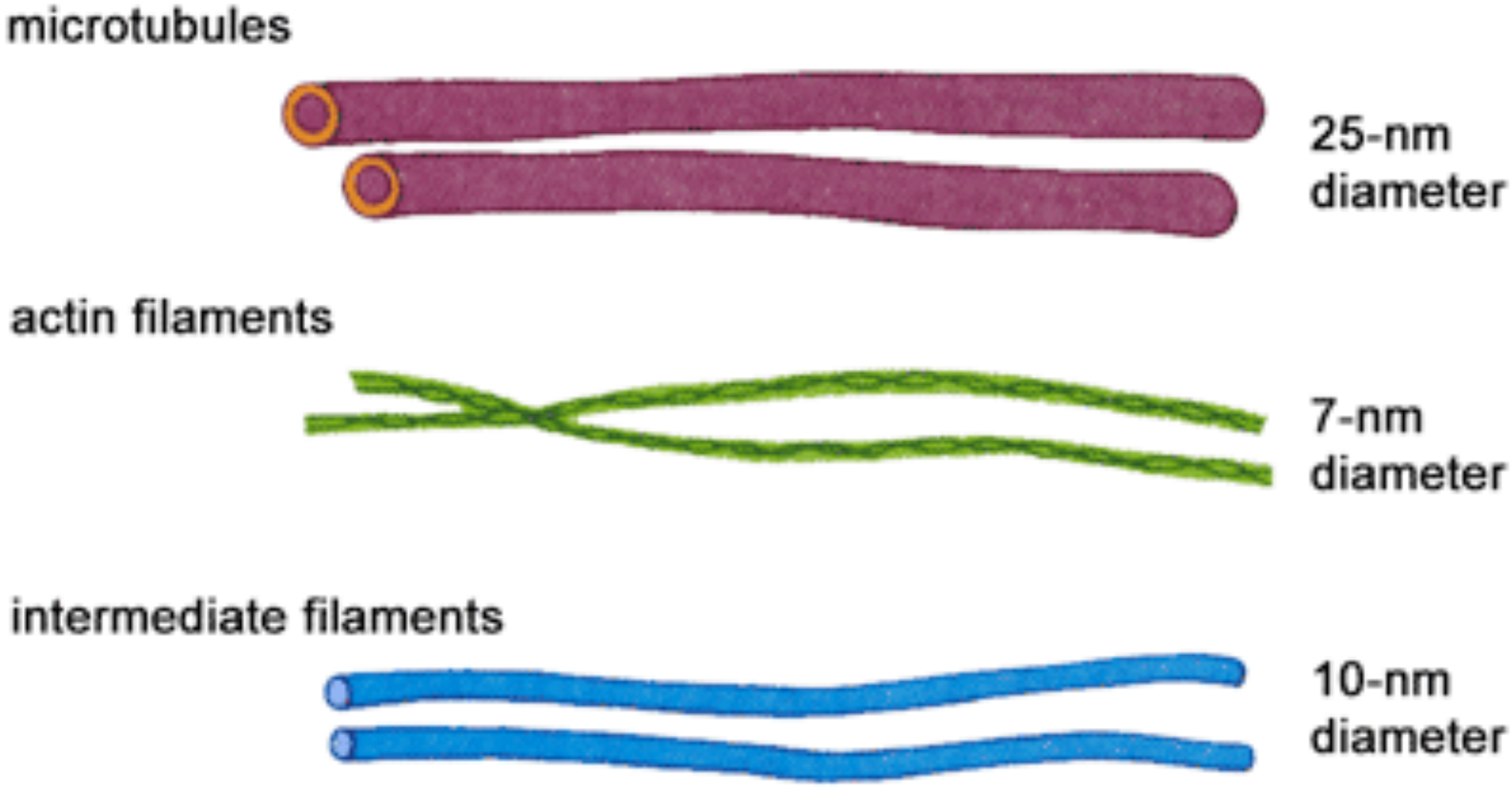

http://library.thinkquest.org/C004535/cytoskeleton.html

dunkel@math.mit.edu

Amoeba

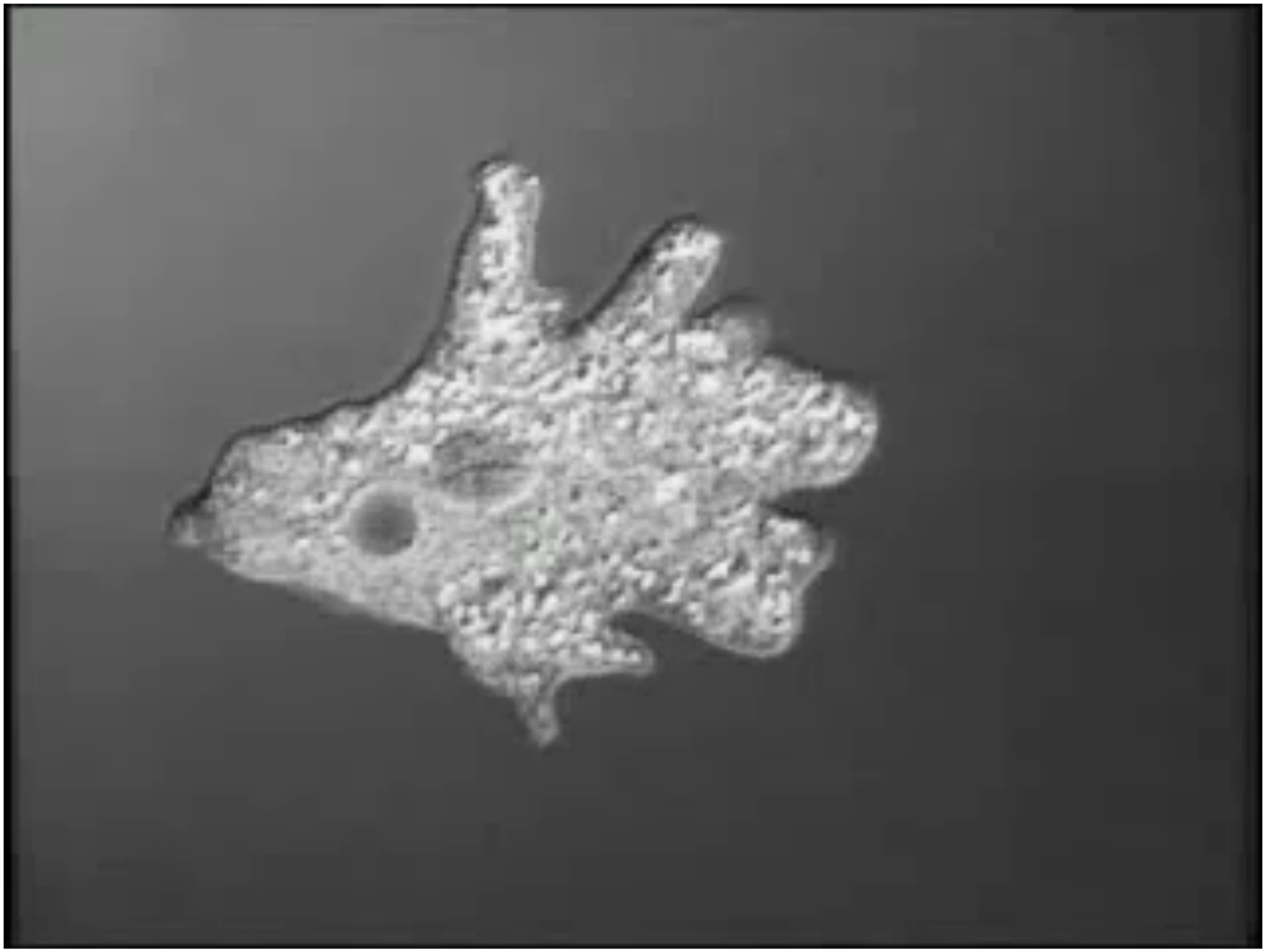

Actin bundles

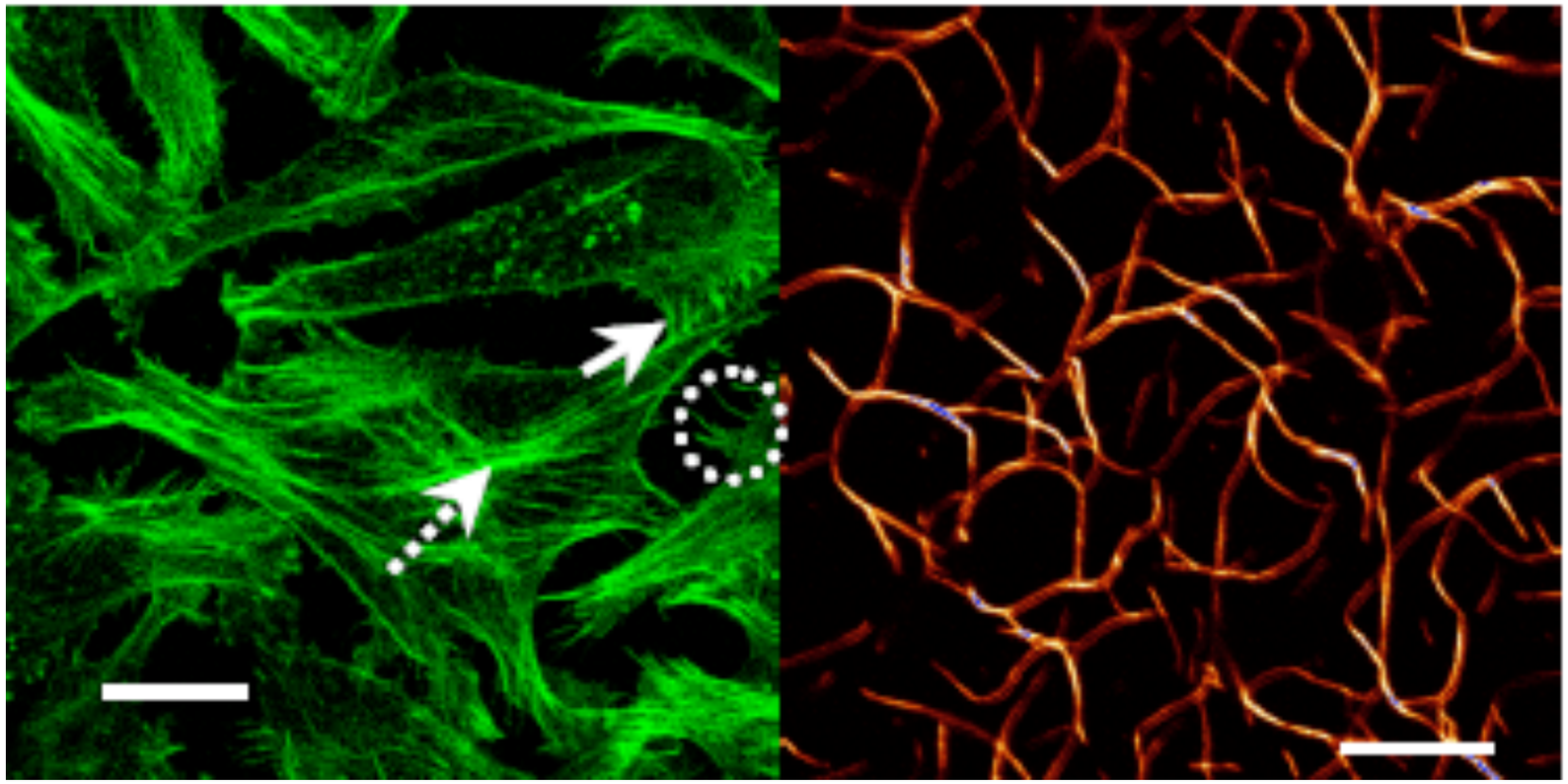

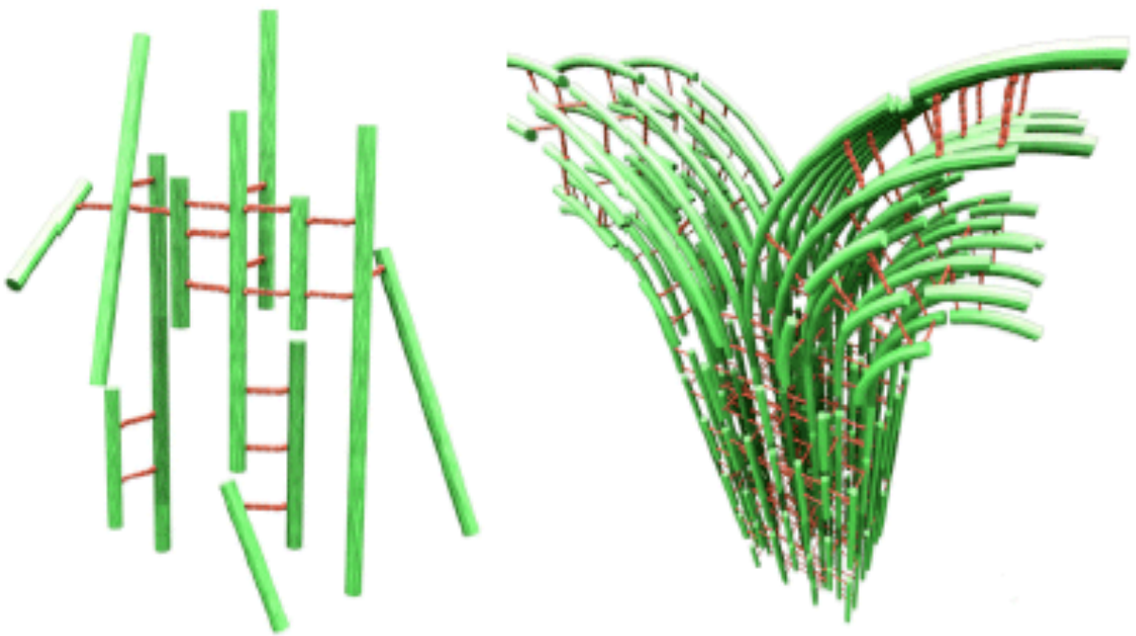

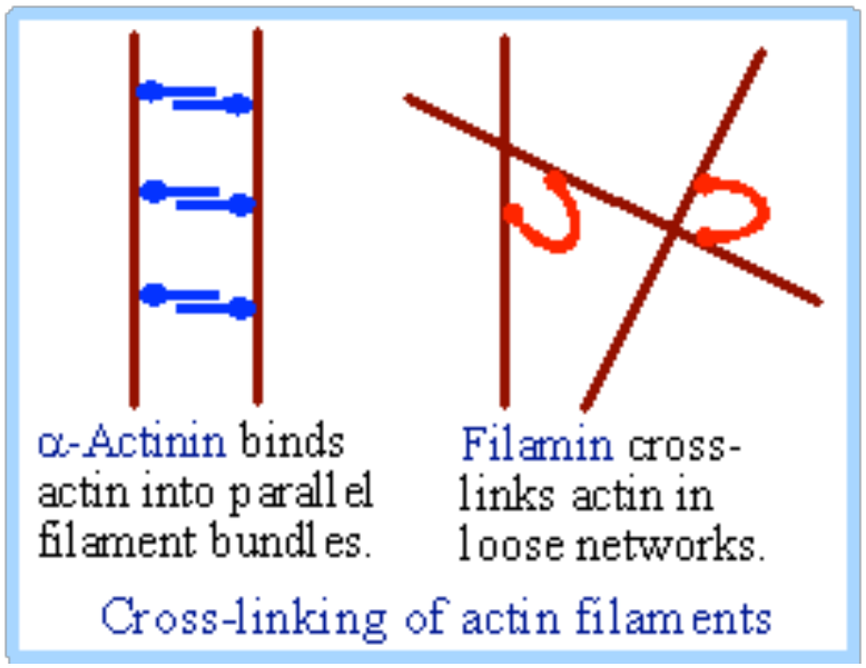

http://www-ssrl.slac.stanford.edu/research/highlights_archive/actinin.html

dunkel@math.mit.edu

Cyto-skeleton

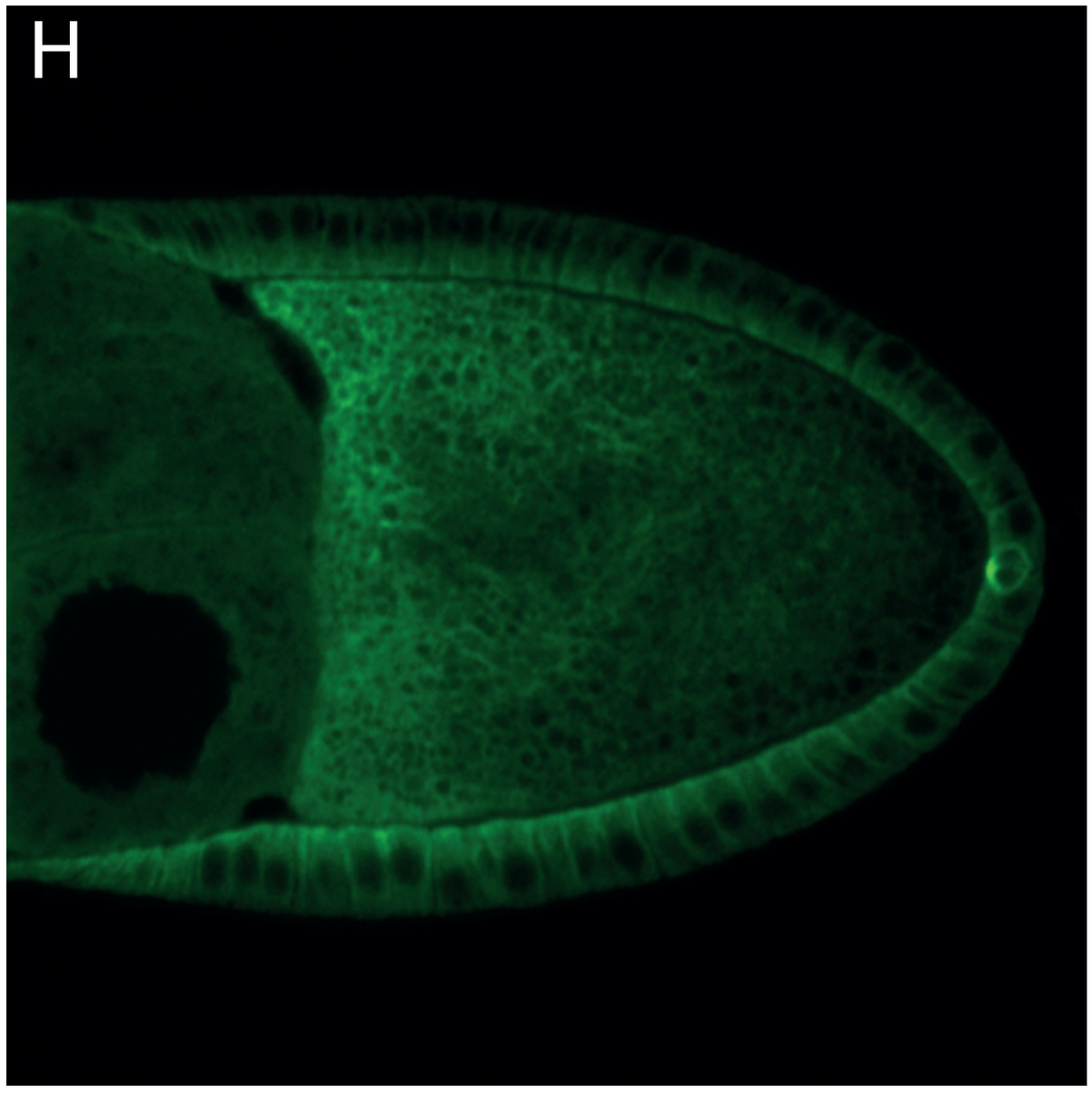

photo:
Philipp Khuc- Trong

Microtubuli network in Drosophila embryo

dunkel@math.mit.edu

Polymers & filaments

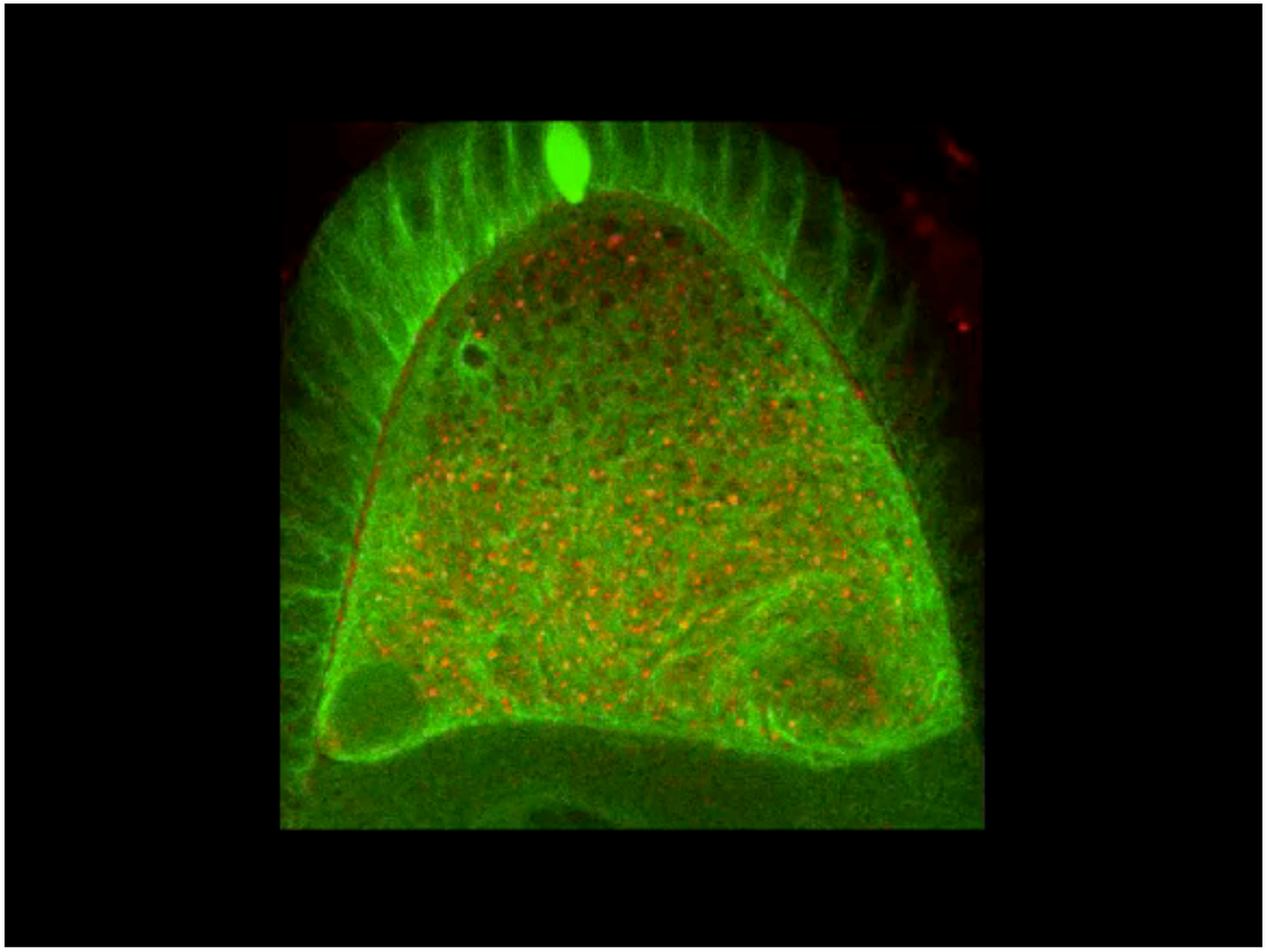

Drosophila oocyte

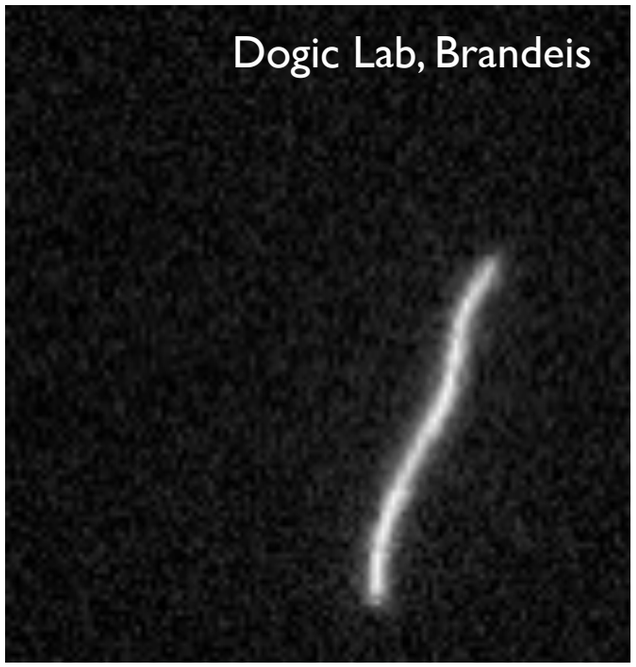

Physical parameters (e.g. bending rigidity) from fluctuation analysis

dunkel@math.mit.edu

Actin in 2D

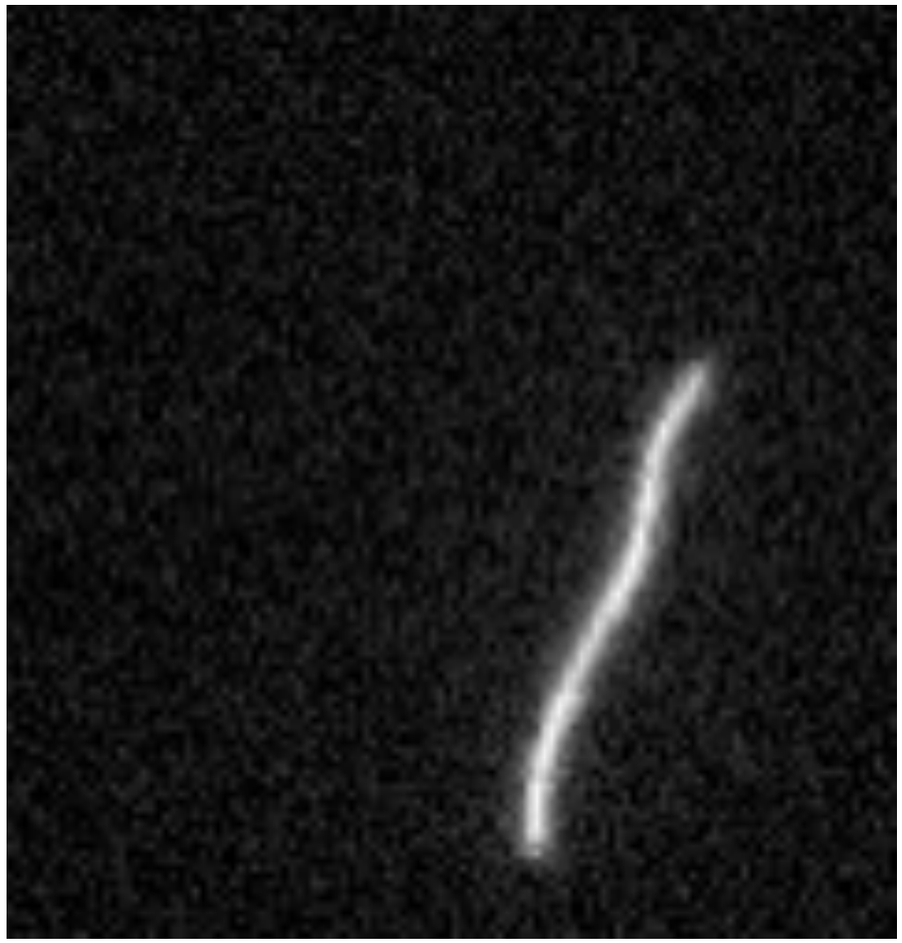

Dogic Lab (Brandeis)

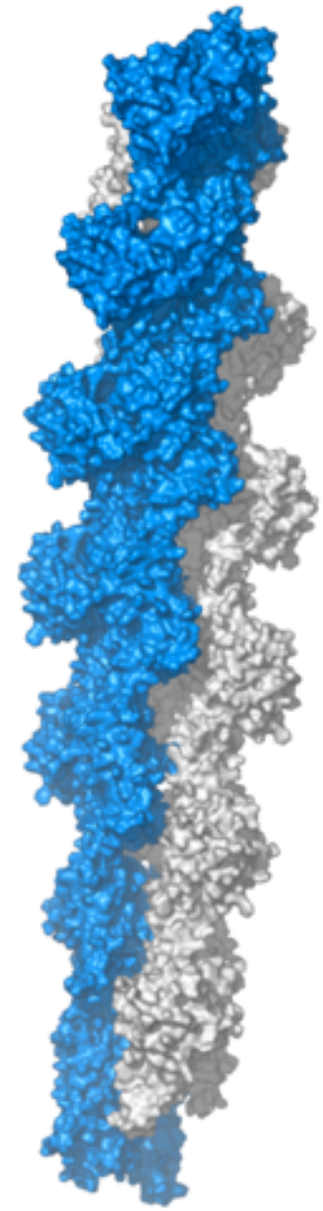

F-Actin

helical filament

dunkel@math.mit.edu

Actin in 2D

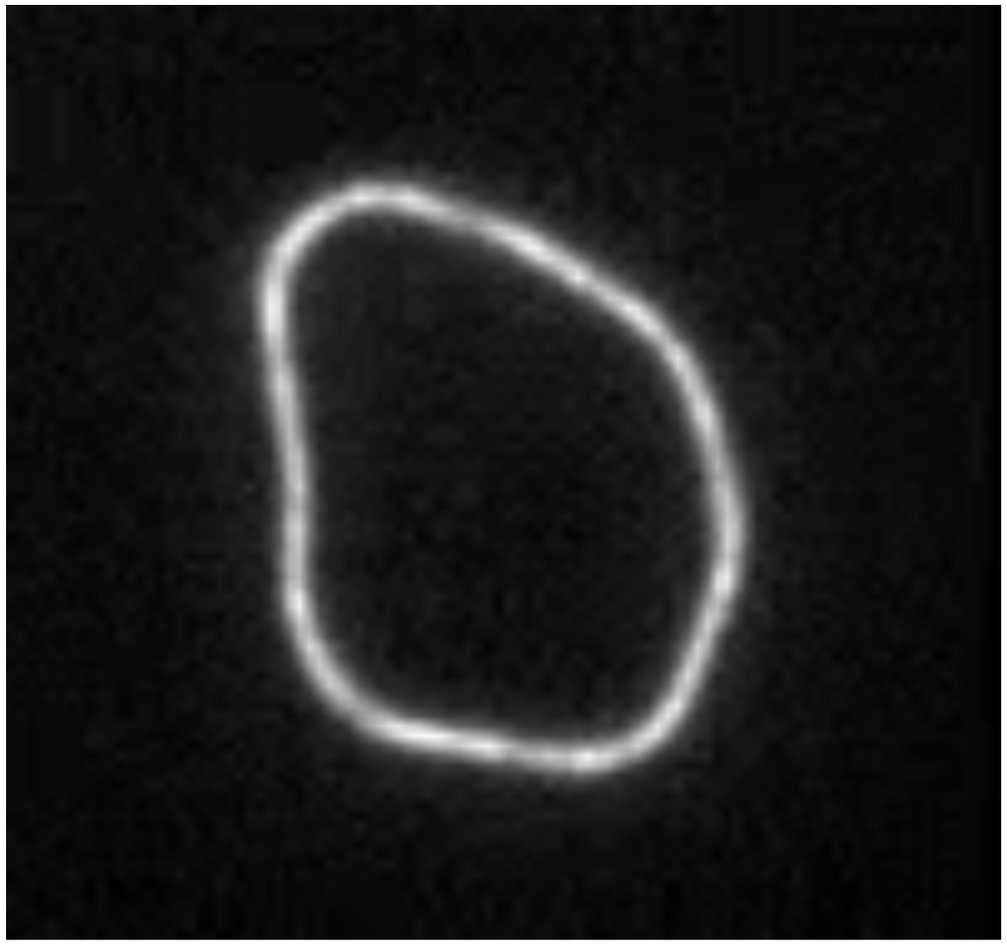

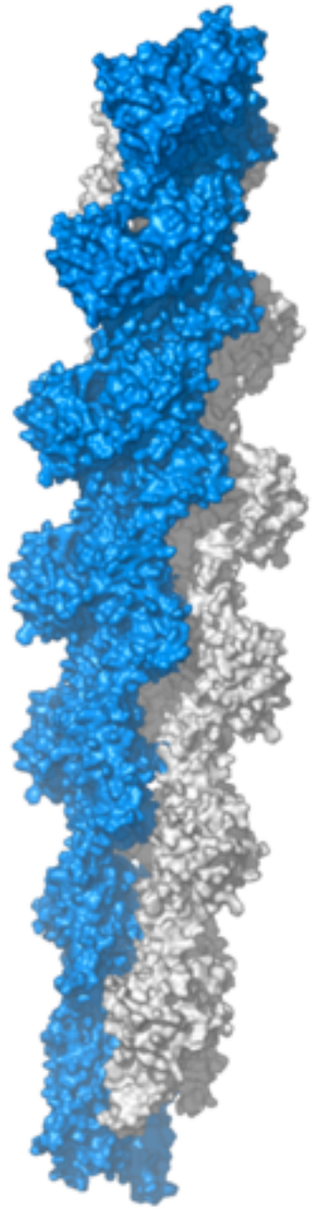

F-Actin

helical filament

Dogic Lab (Brandeis)

dunkel@math.mit.edu

Actin in 2D

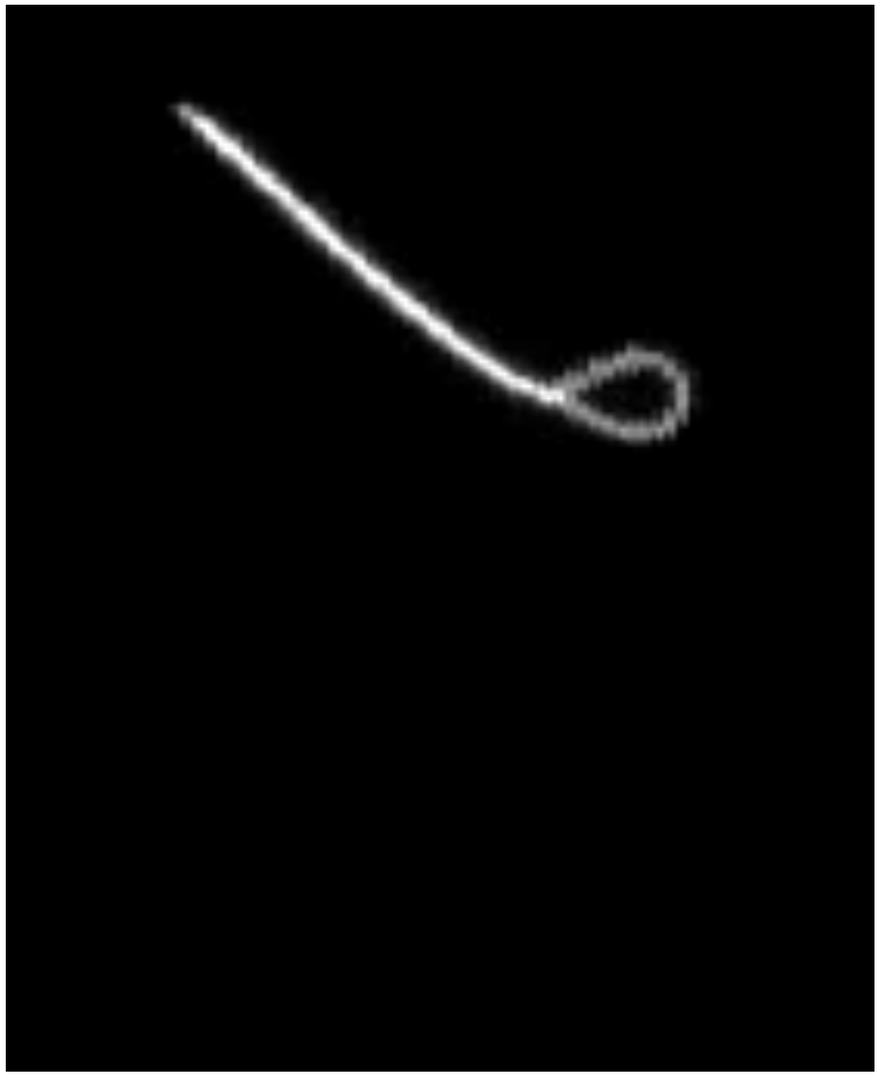

with attractive solvent

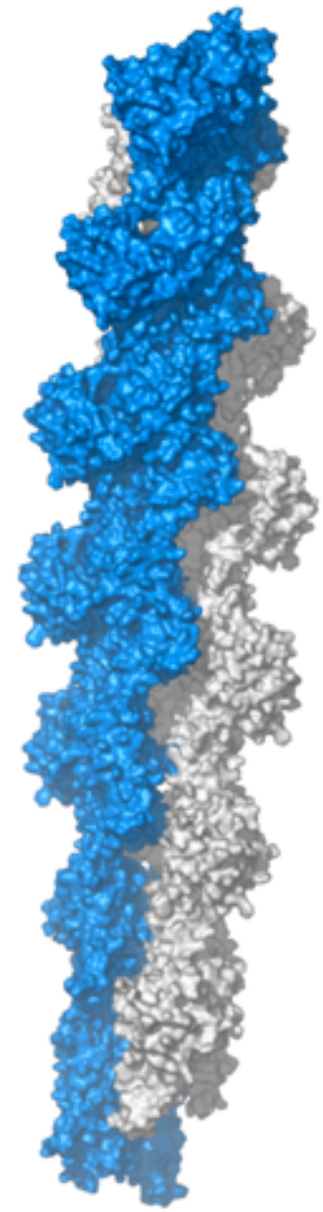

F-Actin

helical filament

Dogic Lab (Brandeis)

dunkel@math.mit.edu

Actin in flow

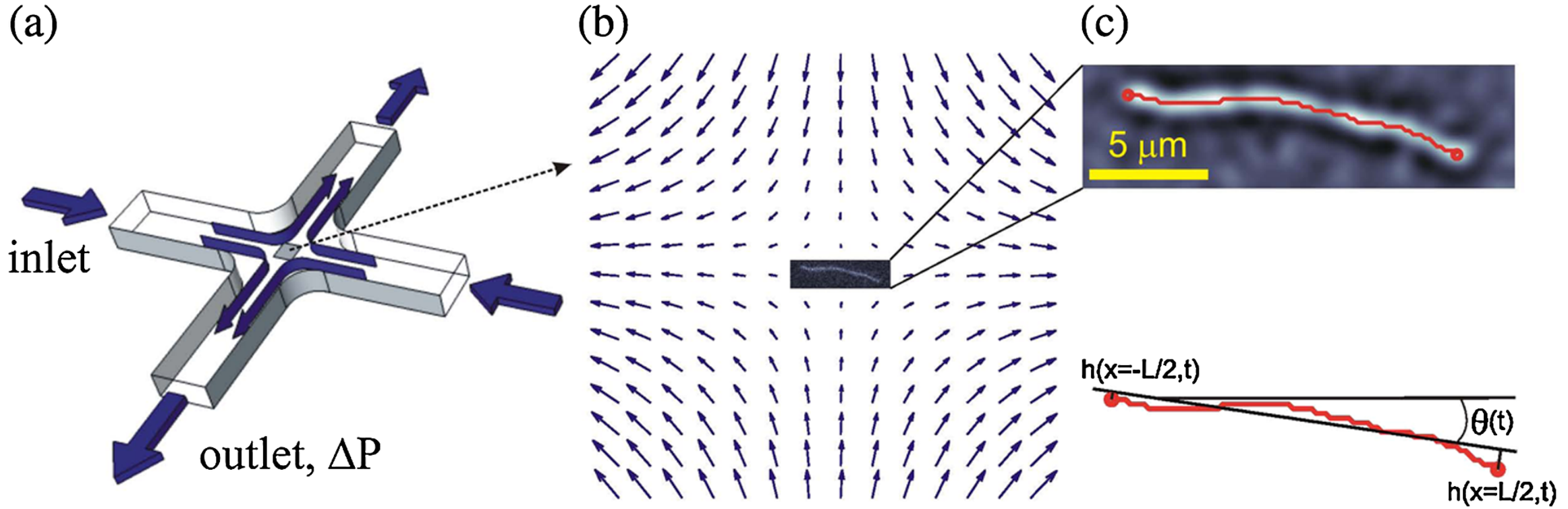

FIG. 1 (color online). Experimental setup. (a) Microfluidic cross-flow geometry controlled by a pressure difference ΔP between inlet and outlet branches. (b) Close-up of the velocity field near the stagnation point, showing a typical actin filament. (c) Raw contour (red) of an actin filament and definition of geometric quantities used in the analysis.

Kantsler & Goldstein (2012) PRL

dunkel@math.mit.edu

Actin in flow

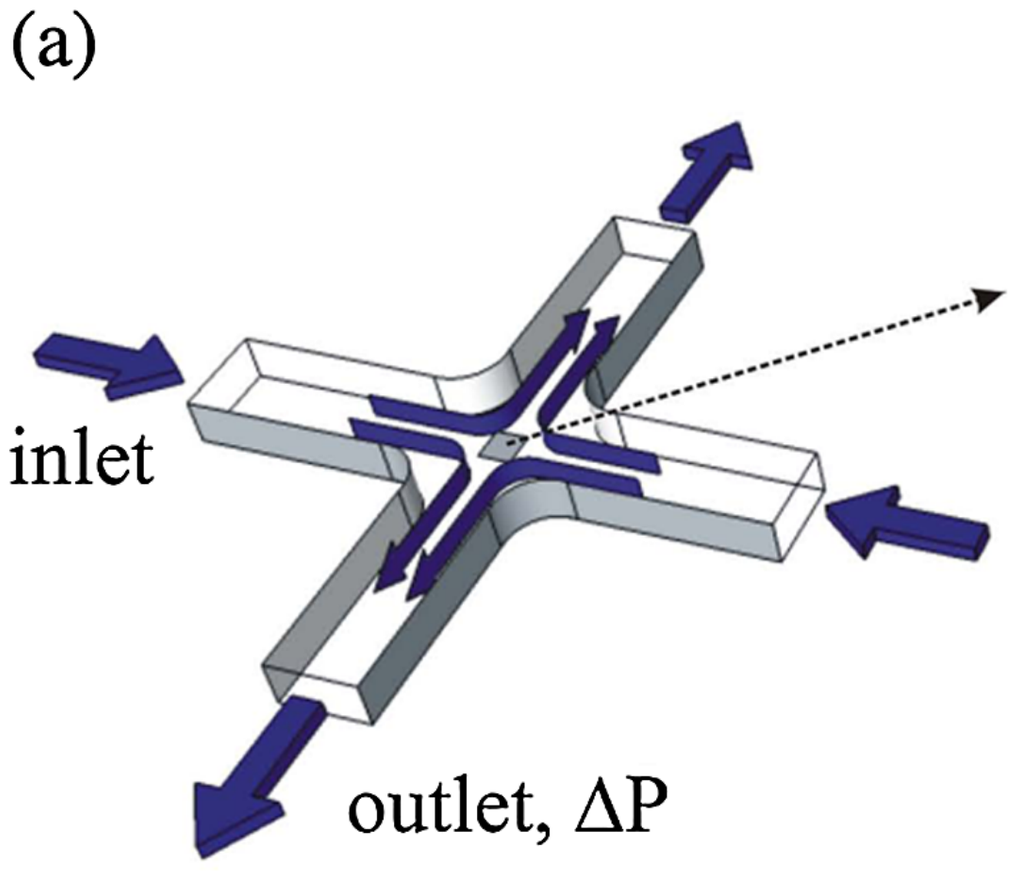

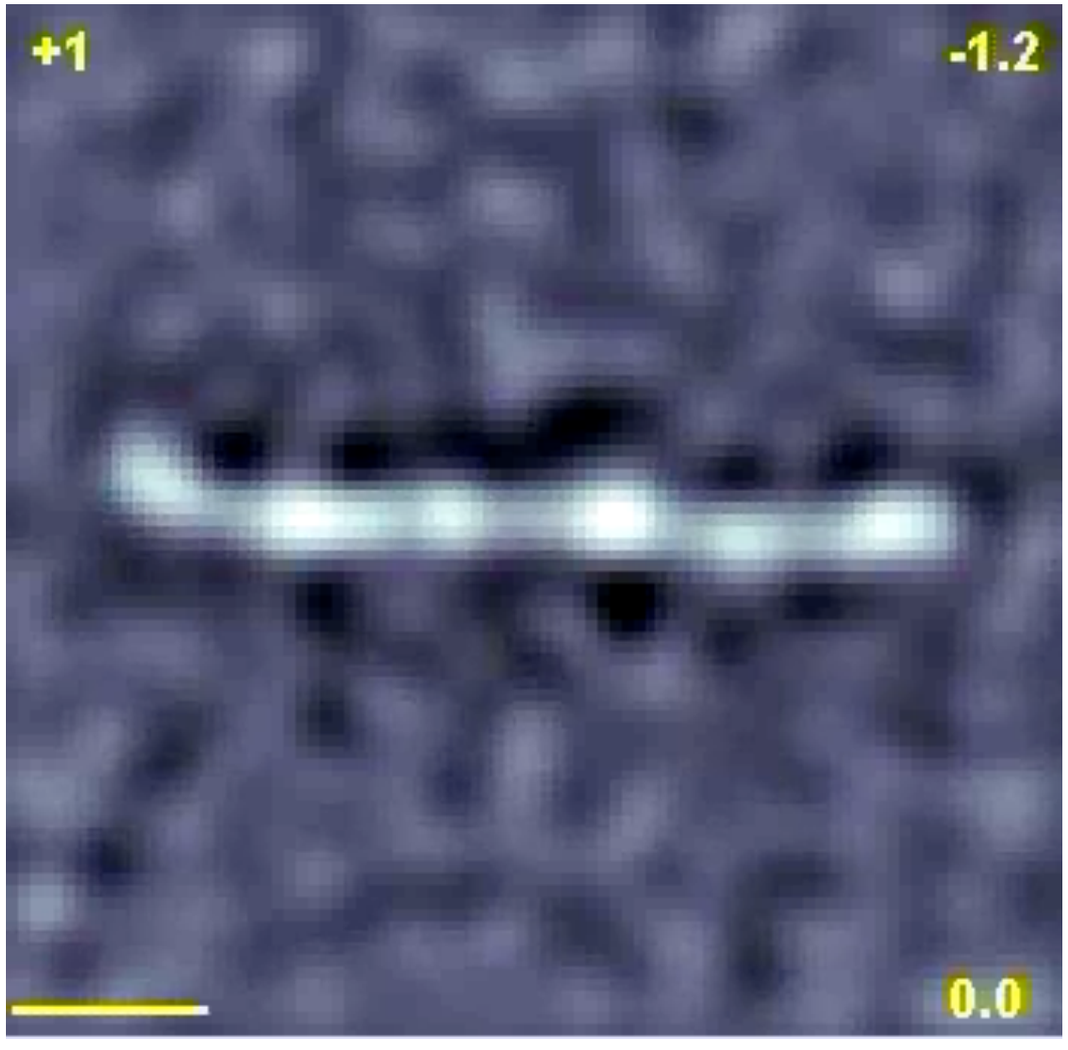

Kantsler & Goldstein (2012) PRL

dunkel@math.mit.edu

Actin in flow

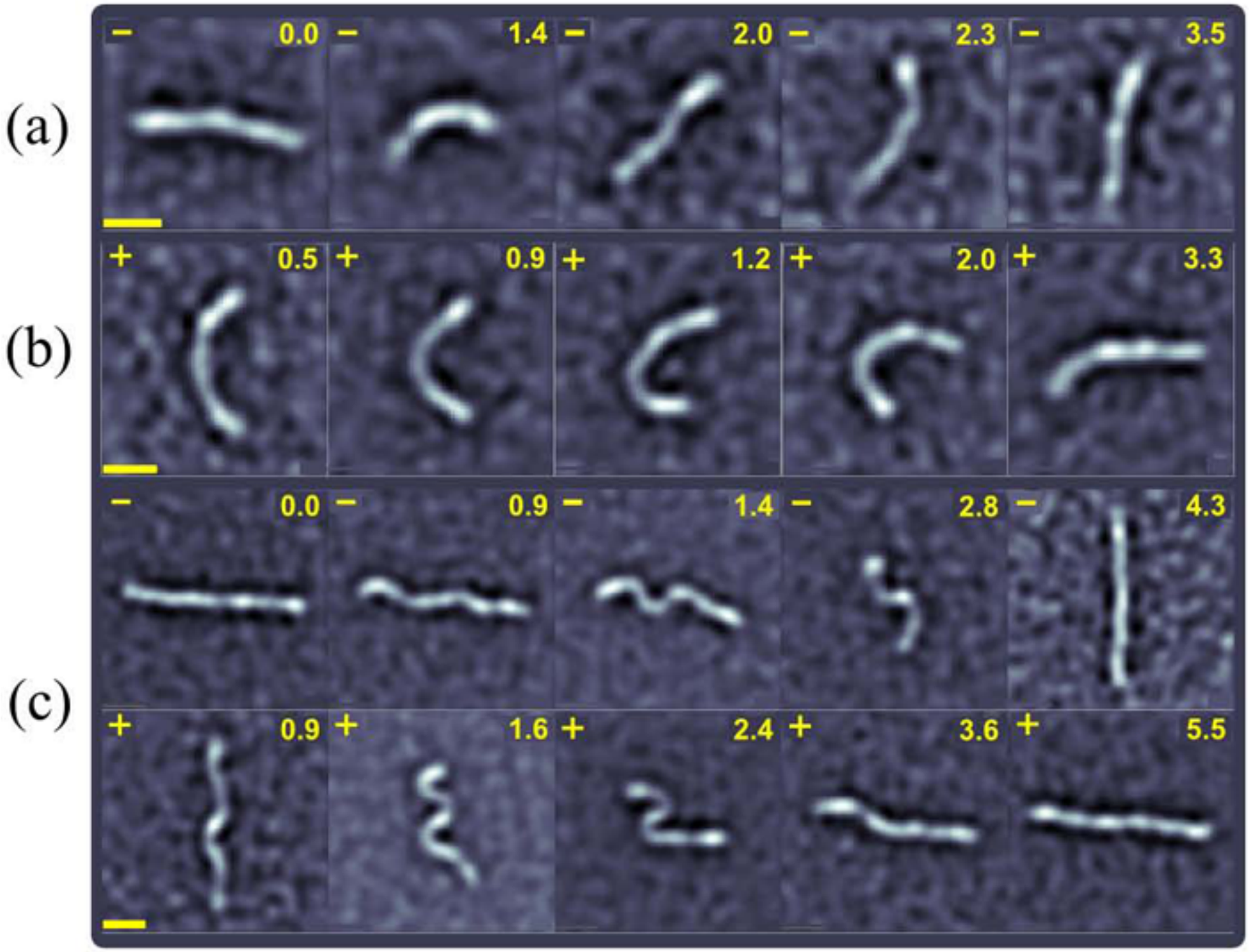

Kantsler & Goldstein (2012) PRL

dunkel@math.mit.edu

Theory

$$\mathcal{E} = \frac{1}{2}\int_{-L/2}^{L/2} dx\{Ah_{xx}^2 + \sigma(x)h_x^2\}, \tag{1}$$

where subscripts indicate differentiation. The *nonuniform* tension induced by the flow [19],

$$\sigma(x) = \frac{2\pi\mu\dot{\gamma}}{\ln(1/\epsilon^2 e)}(L^2/4 - x^2), \tag{2}$$

dunkel@math.mit.edu

Theory

of eigenfunctions $W^{(n)}$ (and eigenvalues λ_n) with boundary conditions $W_{xx}(\pm L/2) = W_{xxx}(\pm L/2) = 0$ [3,21]. Under the convenient rescaling $\xi = \pi x/L$, these obey

$$W^{(n)}_{4\xi} - \Sigma\partial_\xi[(\pi^2/4 - \xi^2)W^{(n)}_\xi] = \Lambda_n W^{(n)}. \qquad (3)$$

The eigenvalues $\Lambda_n = L^4\lambda_n/\pi^4 A$ are functions of [22]

$$\Sigma = \frac{2\mu\dot{\gamma}L^4}{\pi^3 A \ln(1/\epsilon^2 e)}. \qquad (4)$$

When $\Sigma = 0$, the $W^{(n)}$ are eigenfunctions of the one-dimensional biharmonic equation

$$W_{\Sigma=0} = A\sin kx + B\sinh kx + D\cos kx + E\cosh kx. \quad (5)$$

dunkel@math.mit.edu

Theory vs. experiment

(and we assume they are normalized). Equipartition then yields $\langle a_m a_n \rangle = \delta_{mn} L^4 / \pi^4 \ell_p \Lambda_n$, and the local variance $V(x) = \langle [h(x) - \bar{h}]^2 \rangle$ is

$$V(x;\Sigma) = \frac{L^3}{\ell_p \pi^4} \sum_{n=1}^{\infty} \frac{W^{(n)}(x)^2}{\Lambda_n(\Sigma)}.$$

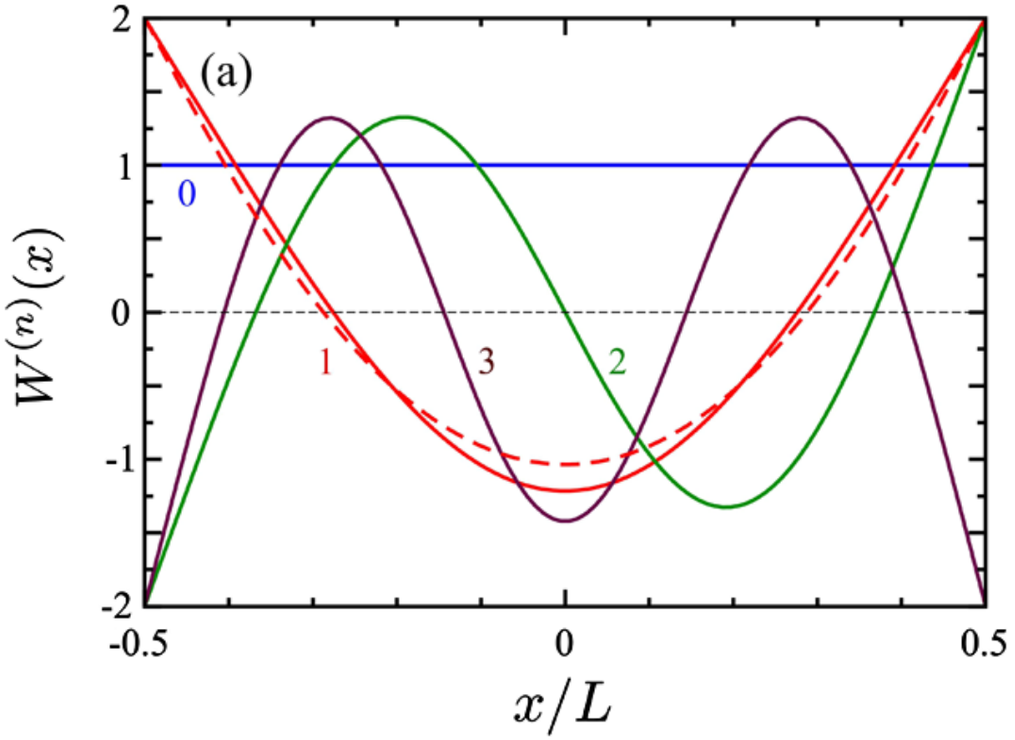

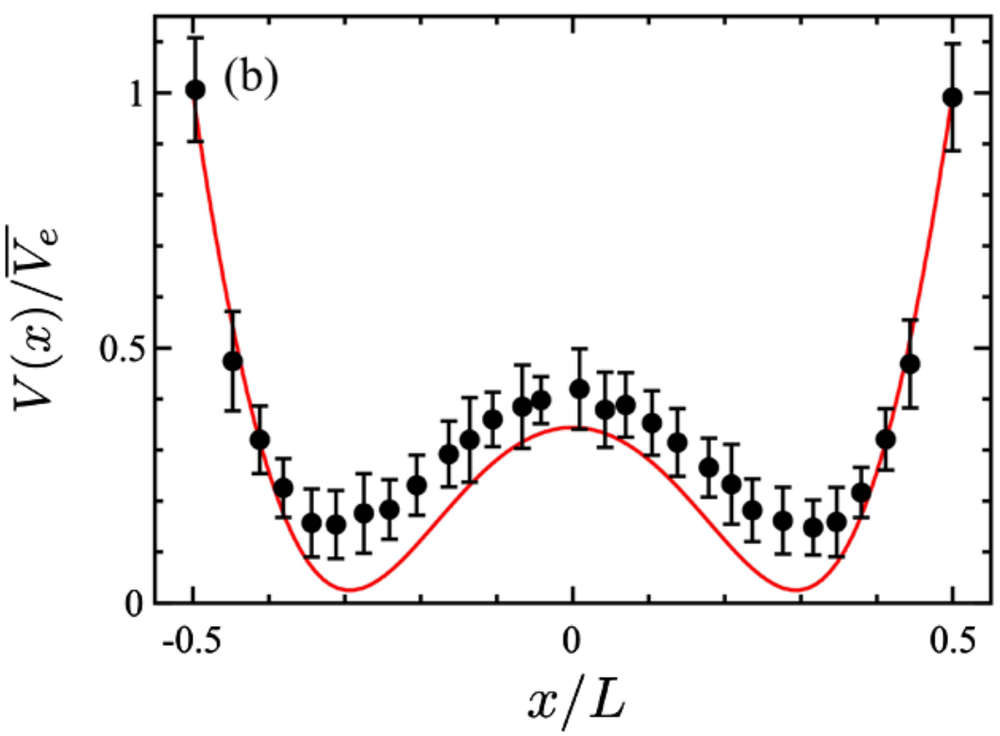

dunkel@math.mit.edu

Bio-technology
&
Soft Active Materials

dunkel@math.mit.edu

DNA Origami - principle

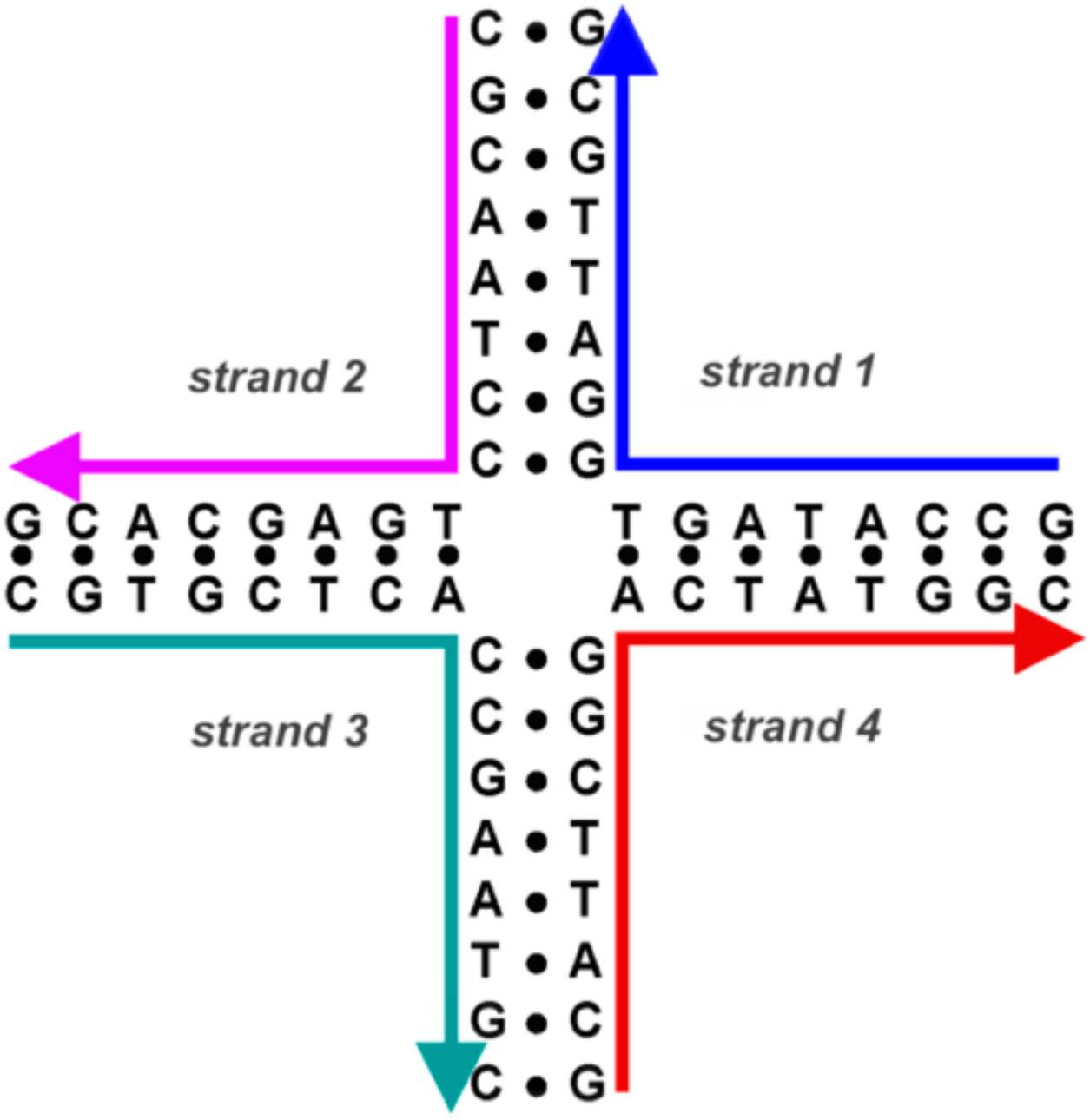

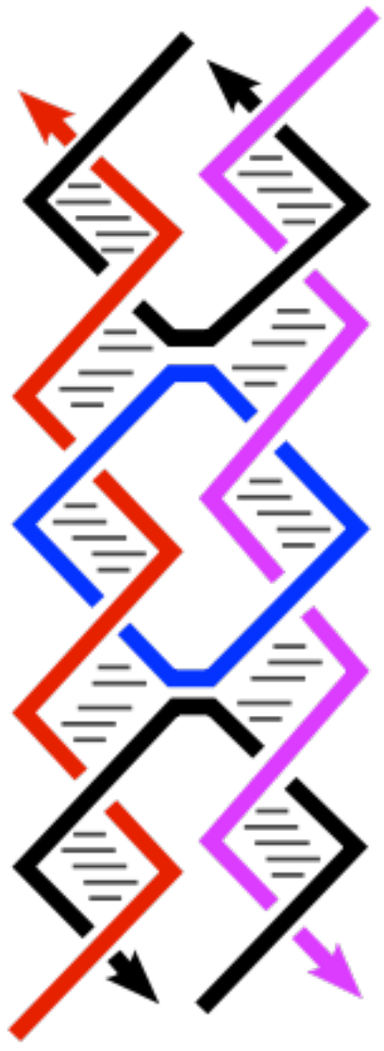

source: wiki

dunkel@math.mit.edu

DNA Origami - principle

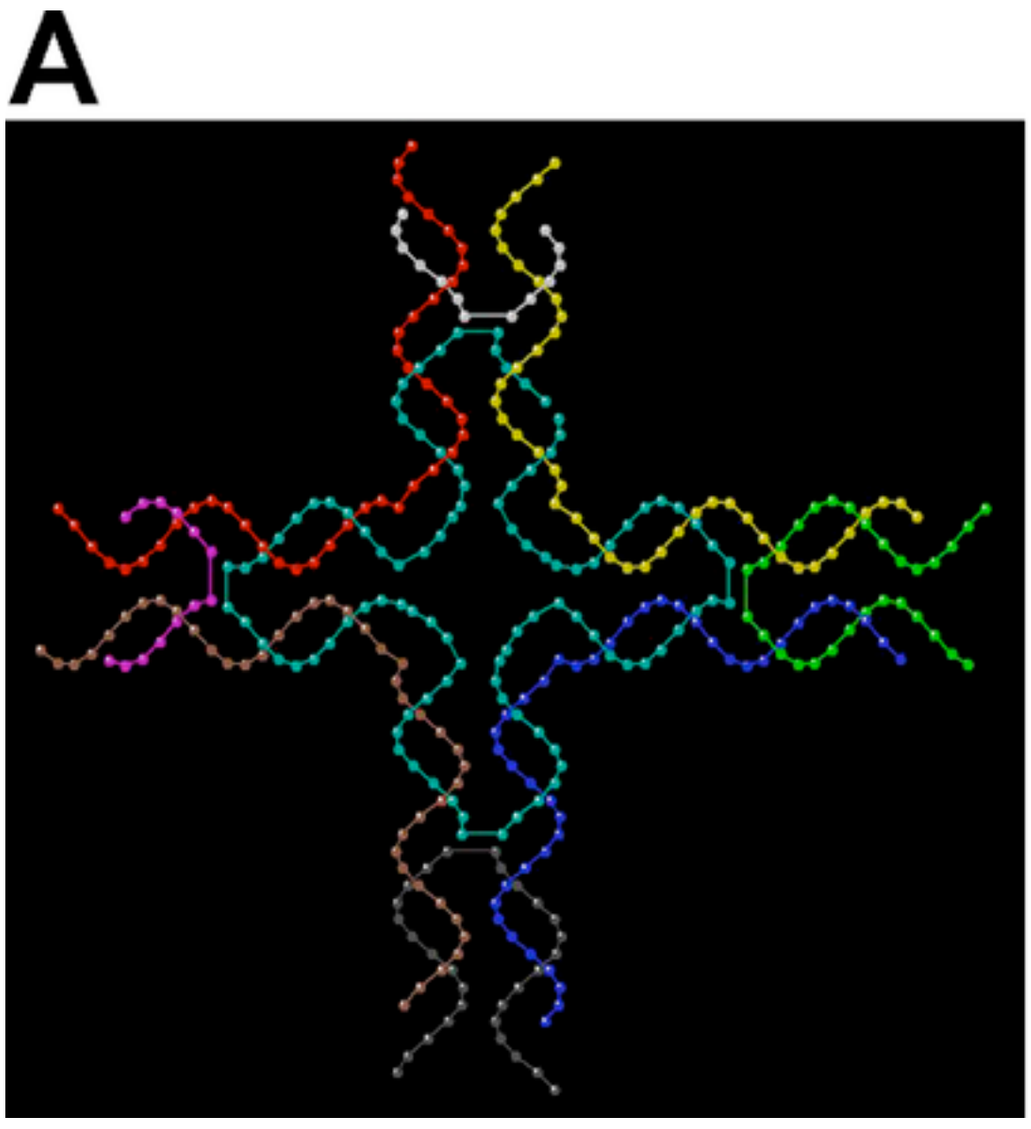

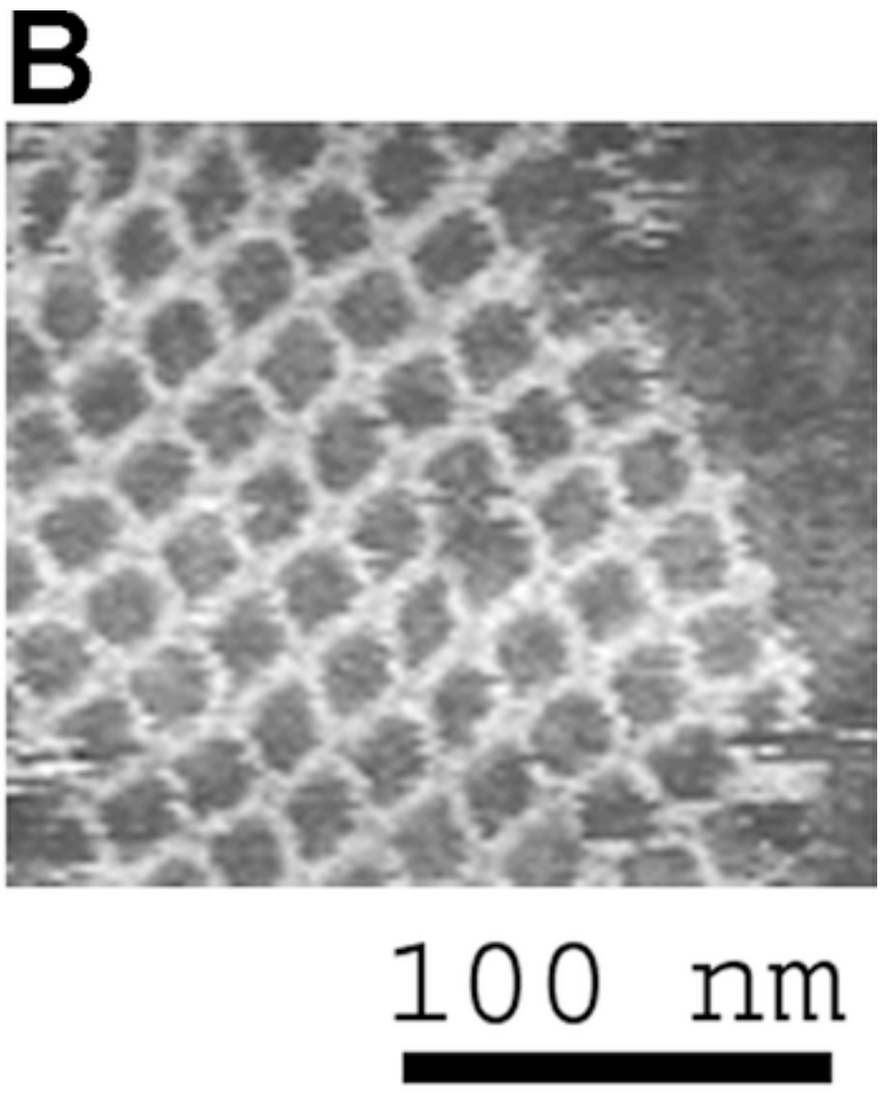

Strong M: *Protein Nanomachines.* PLoS Biol 2/3/2004: e73

dunkel@math.mit.edu

DNA Origami - 2D

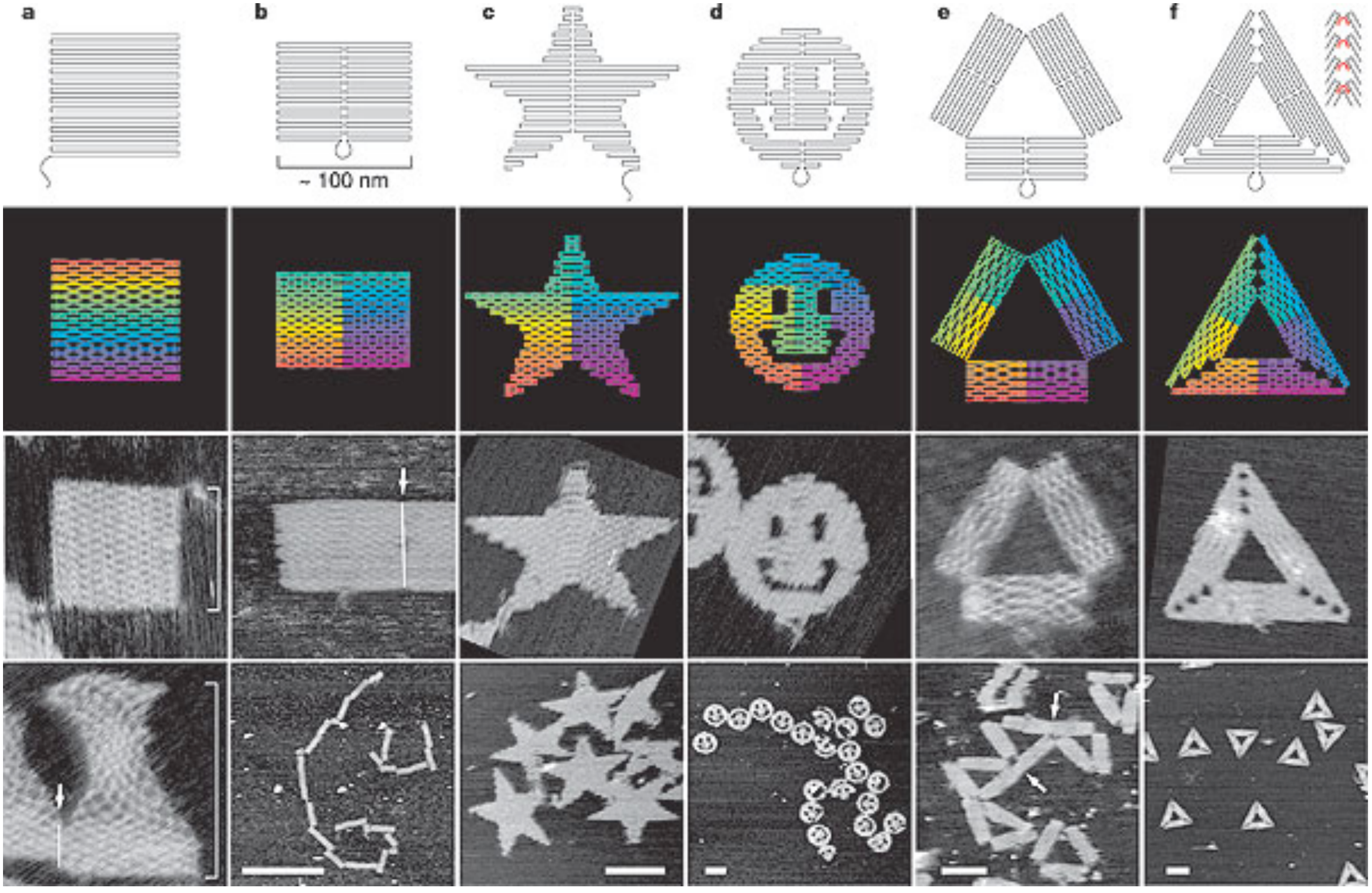

http://www.nature.com/scitable/blog/bio2.0/dna_origami

dunkel@math.mit.edu

DNA Origami - 3D

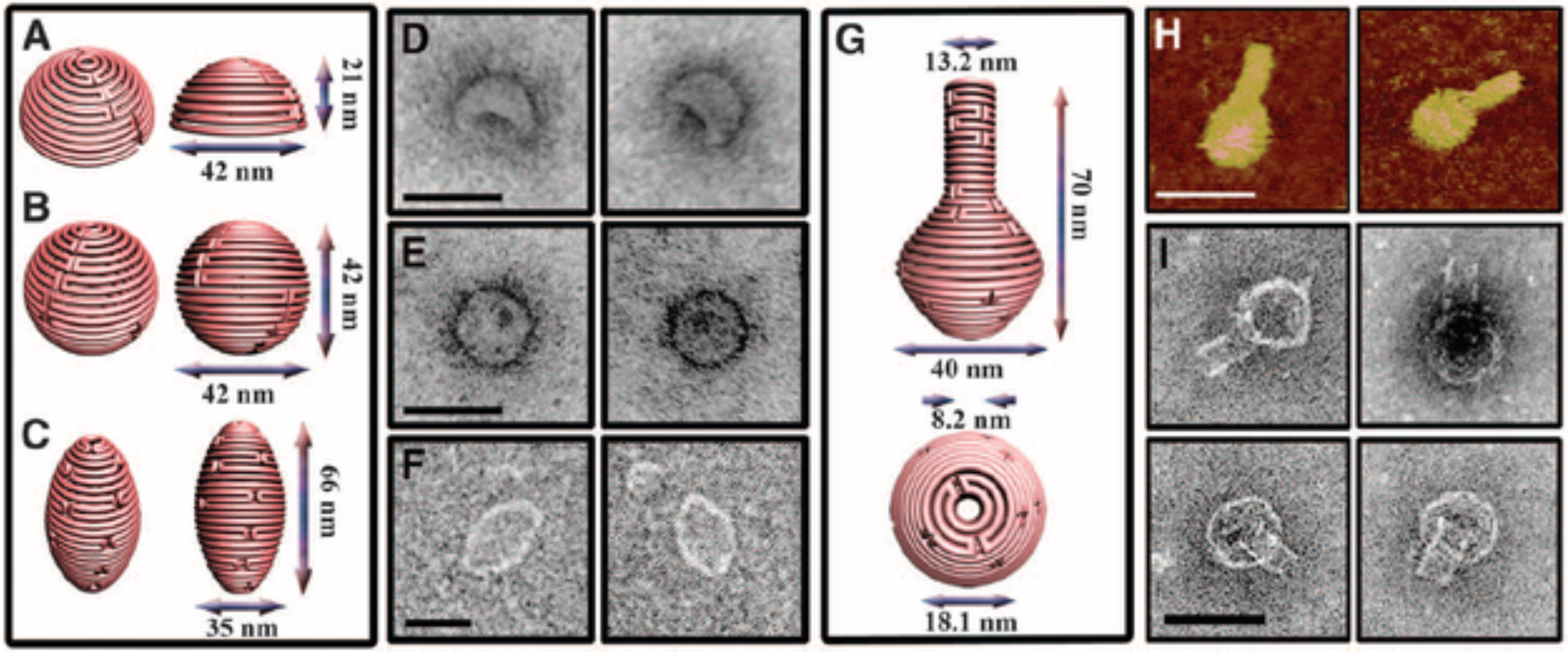

http://www.nature.com/scitable/blog/bio2.0/dna_origami

dunkel@math.mit.edu

DNA polyhedra

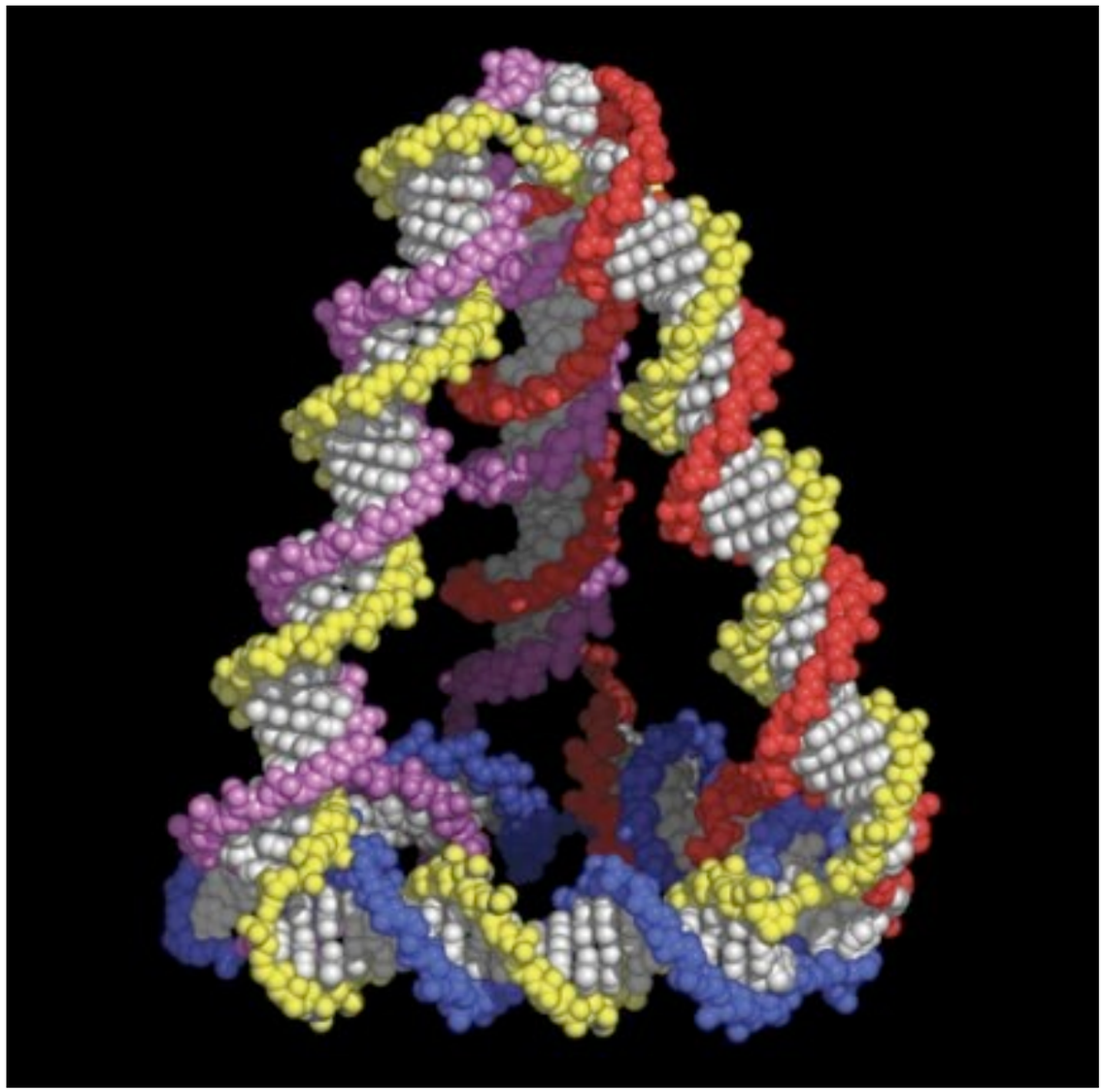

edge ~ 10nm

A rigid tetrahedron formed by self-assembly from DNA, figure from Goodman et al, Science 310 p1661 (2005)

dunkel@math.mit.edu

Computation

Mark Bathe, MIT

http://lcbb.mit.edu/software/index.html

dunkel@math.mit.edu

Artificial cilia

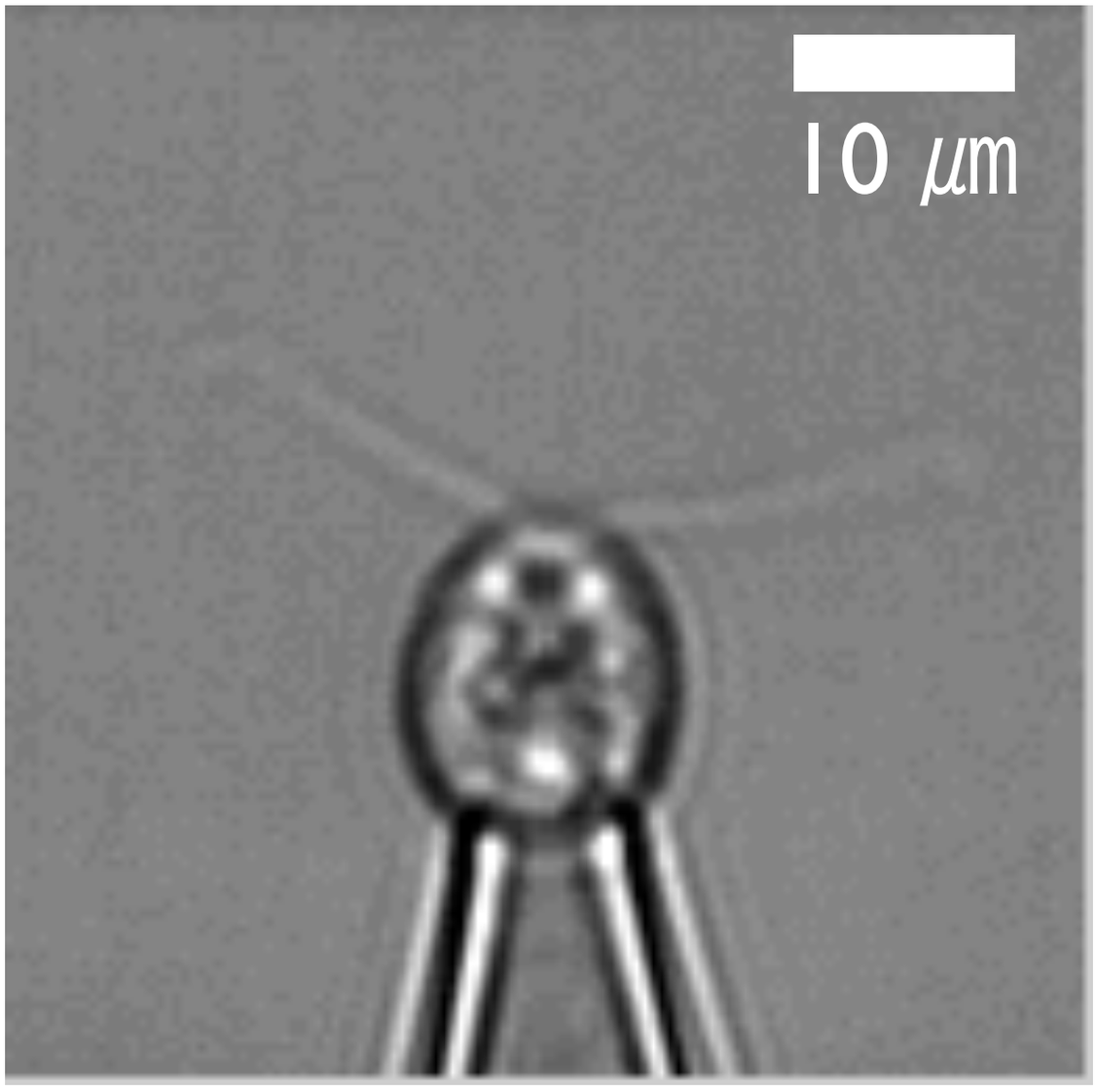

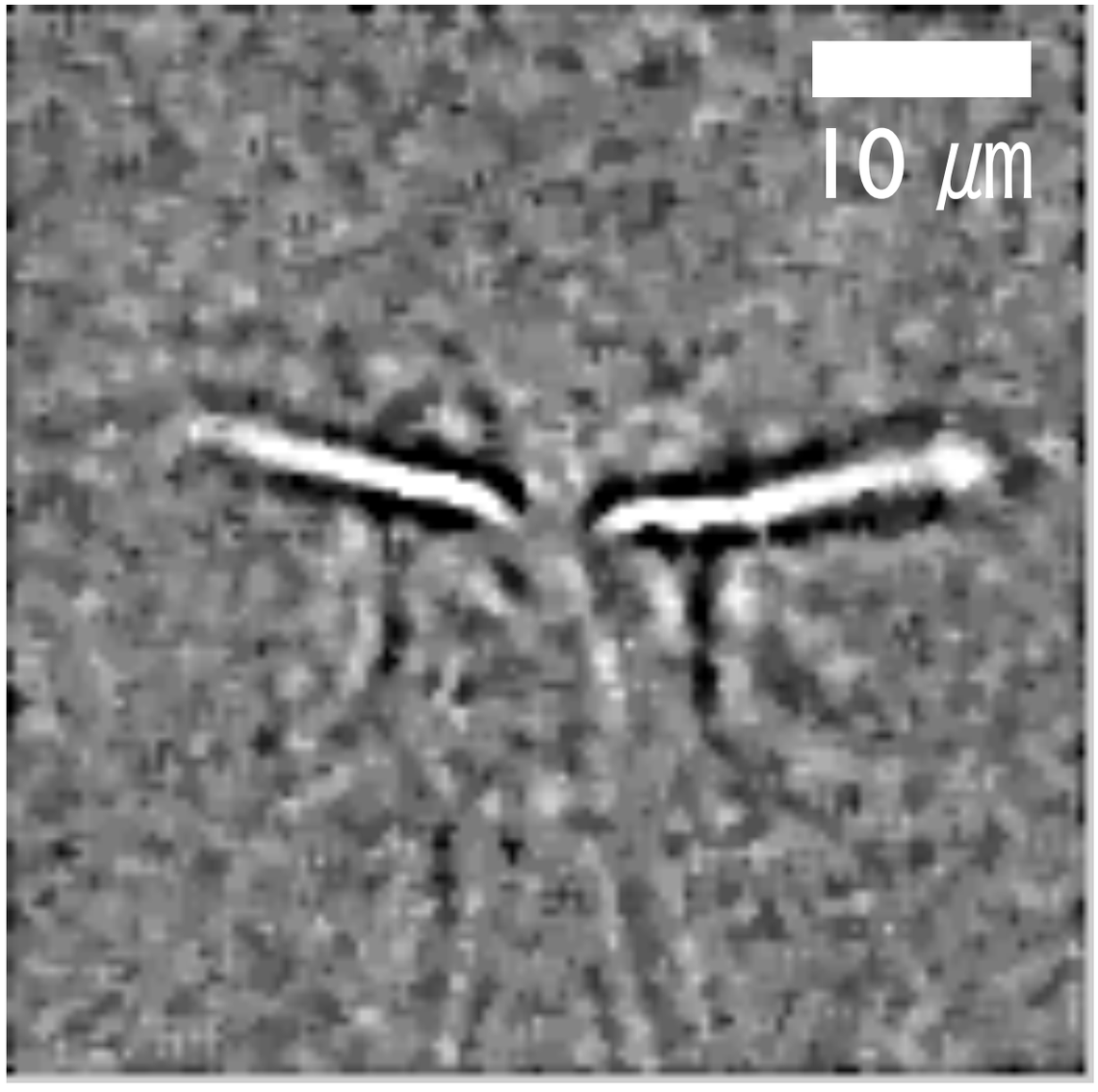

~ 50 beats / sec

speed ~100 μm/s

Goldstein et al (2011) PRL

dunkel@math.mit.edu

Artificial cilia

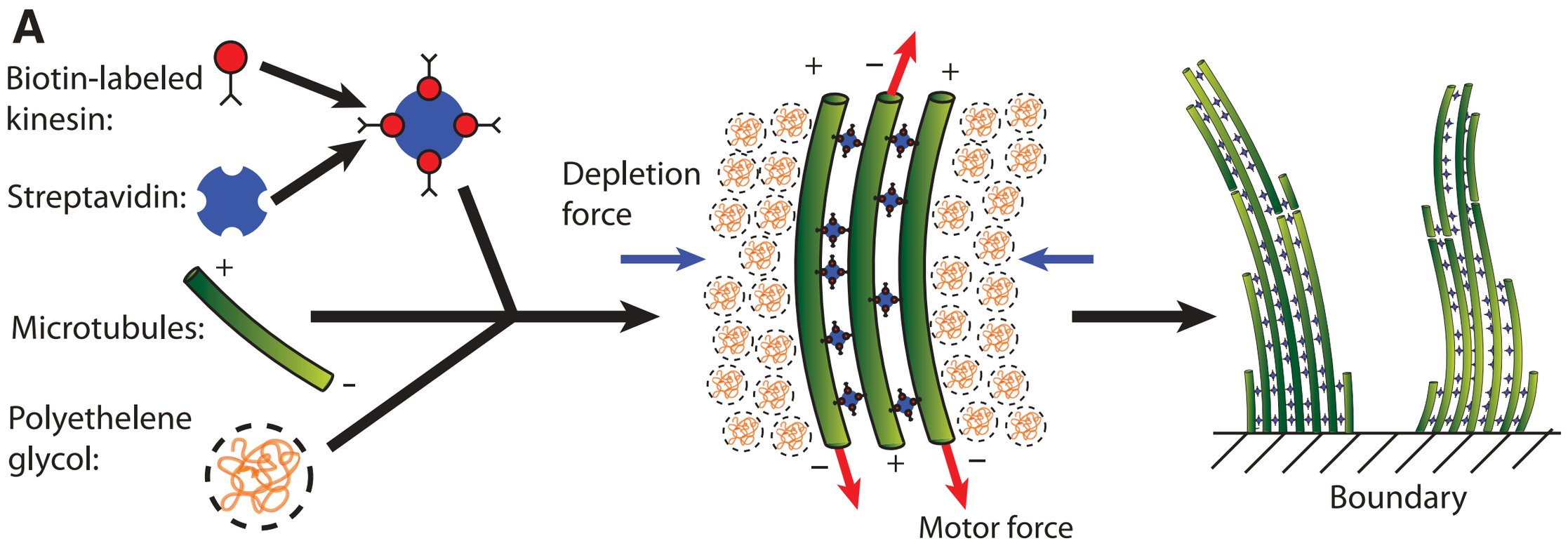

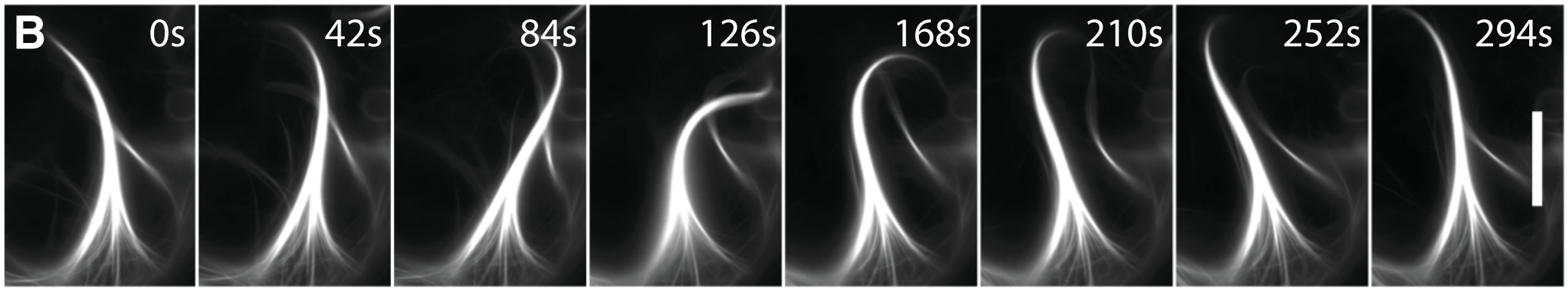

Dogic Lab (Brandeis)

Science 2011

dunkel@math.mit.edu

Artificial cilia

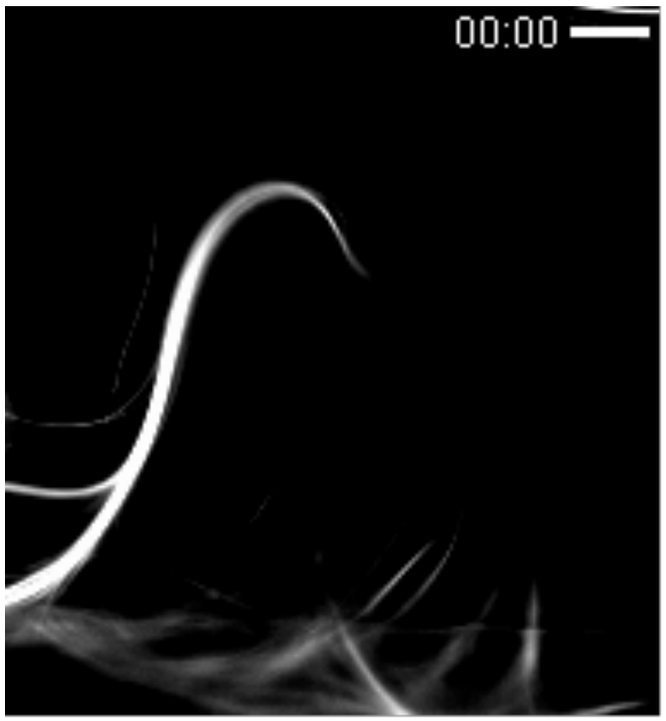

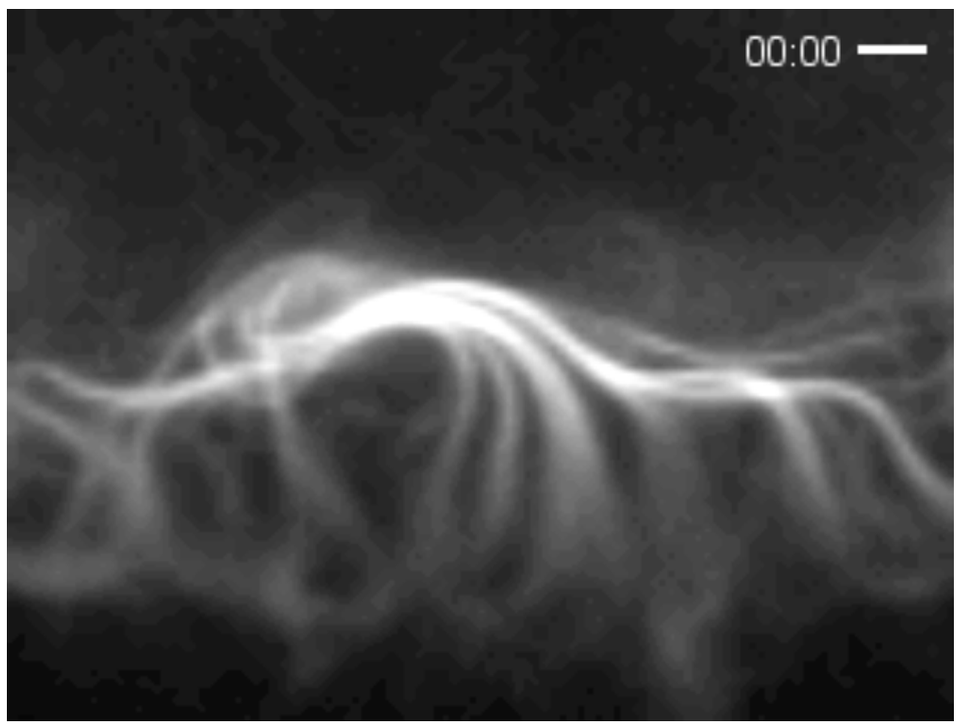

Dogic Lab
(Brandeis)

Science 2011

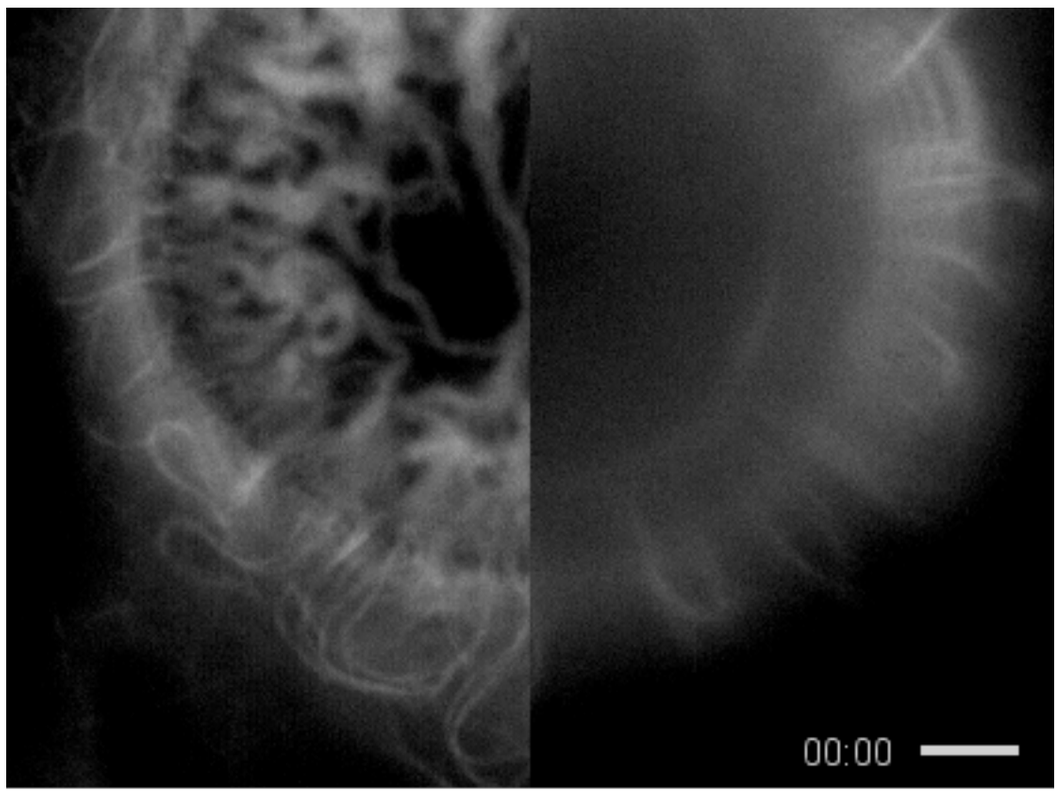

dunkel@math.mit.edu

Basic polymer models

Karjalainen et al (2014) Polym Chem

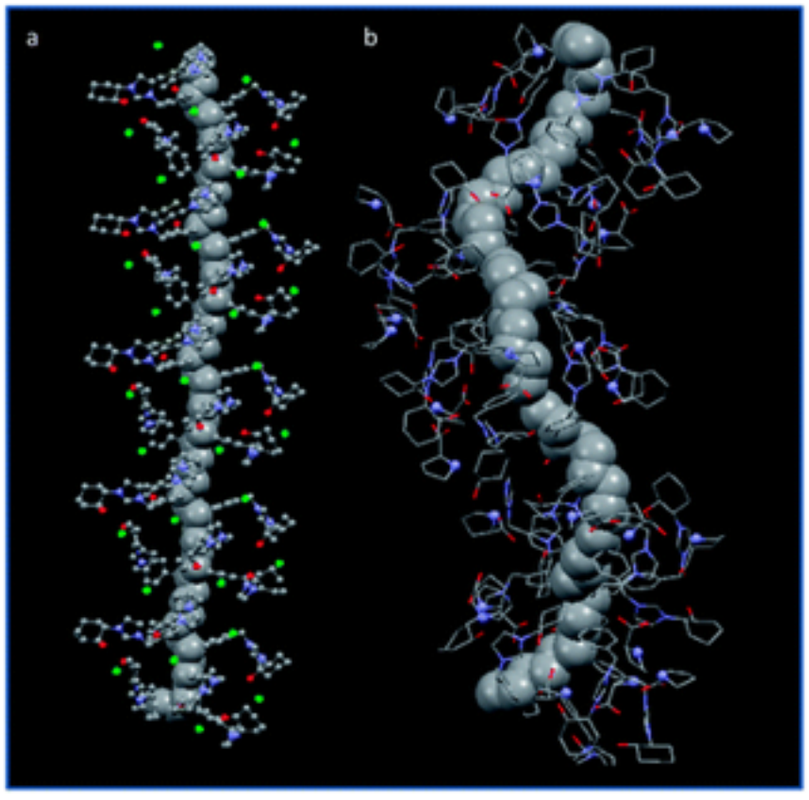

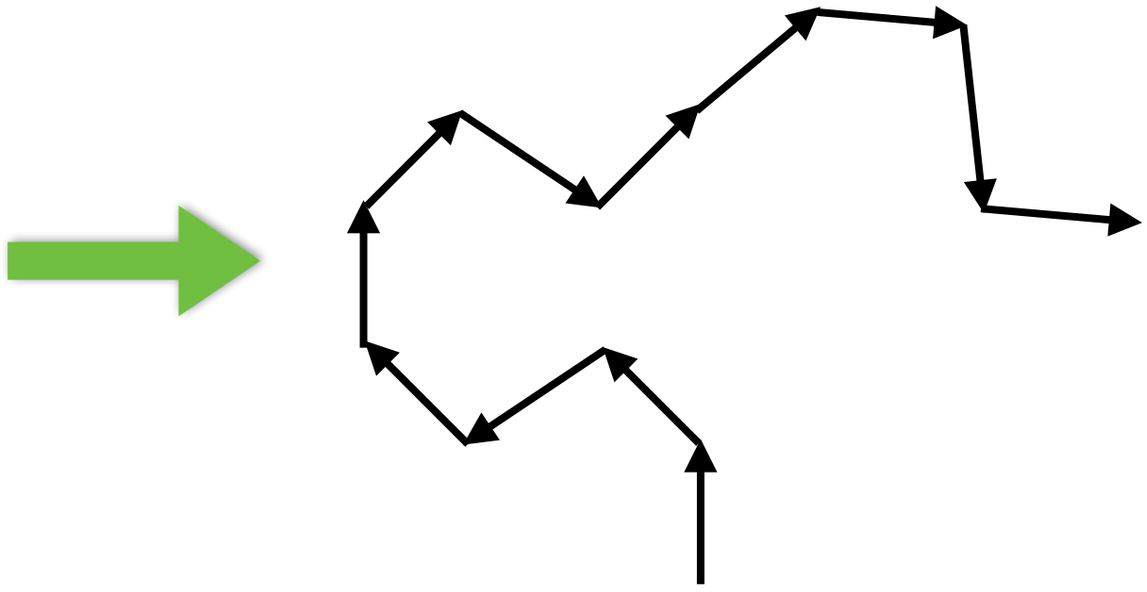

http://dx.doi.org/10.1039/1759-9962/2010

dunkel@math.mit.edu

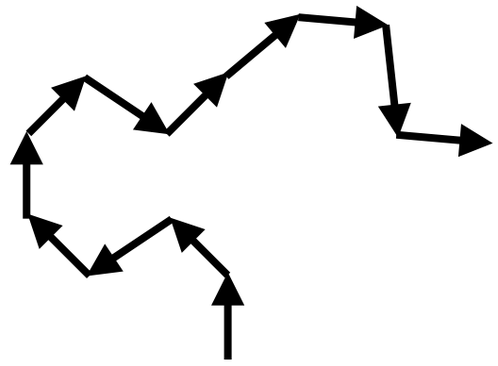

2.1 Persistent random walks

2.1.1 von Mises-Fisher (vMF) distribution

The PDF of the vMF distribution on the unit sphere $\boldsymbol{n} \in \mathbb{S}$ reads

$$f(\boldsymbol{n}|\boldsymbol{\mu}) = C_2 e^{\kappa \boldsymbol{n}\cdot\boldsymbol{\mu}}. \tag{2.1}$$

The parameter $\boldsymbol{\mu} \in \mathbb{S}$ determines the mean direction and $\boldsymbol{\kappa}$ the spread, with $\kappa = 0$ corresponding to a uniform distribution and $\kappa \to \infty$ to a δ-distribution at $\boldsymbol{n} = \boldsymbol{\mu}$. Assuming w.l.o.g. $\boldsymbol{\mu} = (0, 0, 1)$ and using spherical coordinates $\boldsymbol{n} = (\cos\phi \sin\theta, \sin\phi \sin\theta, \cos\theta)$ with $(\phi, \theta) \in [0, 2\pi) \times [0, \pi]$, the normalization constant C_2 can be computed from

$$\begin{aligned} 1 &= C_2 \int_0^{2\pi} d\phi \int_0^{\pi} d\theta \, \sin\theta \, f(\boldsymbol{n}|\boldsymbol{\mu}) \\ &= C_2 \int_0^{2\pi} d\phi \int_0^{\pi} d\theta \, \sin\theta \, e^{\kappa\cos\theta} \\ &= C_2 \frac{4\pi \sinh\kappa}{\kappa}, \end{aligned} \tag{2.2}$$

yielding

$$C_2 = \frac{\kappa}{4\pi \sinh\kappa}. \tag{2.3}$$

Similarly, one finds for the mean

$$\mathbb{E}[\boldsymbol{n}|\boldsymbol{\mu}] = C_2 \int dn \, \boldsymbol{n} \, e^{\kappa \boldsymbol{n}\cdot\boldsymbol{\mu}} = \left(\frac{1}{\tanh\kappa} - \frac{1}{\kappa} \right) \boldsymbol{\mu} =: \sigma \boldsymbol{\mu}, \tag{2.4a}$$

dunkel@math.mit.edu

von Mises-Fisher distribution

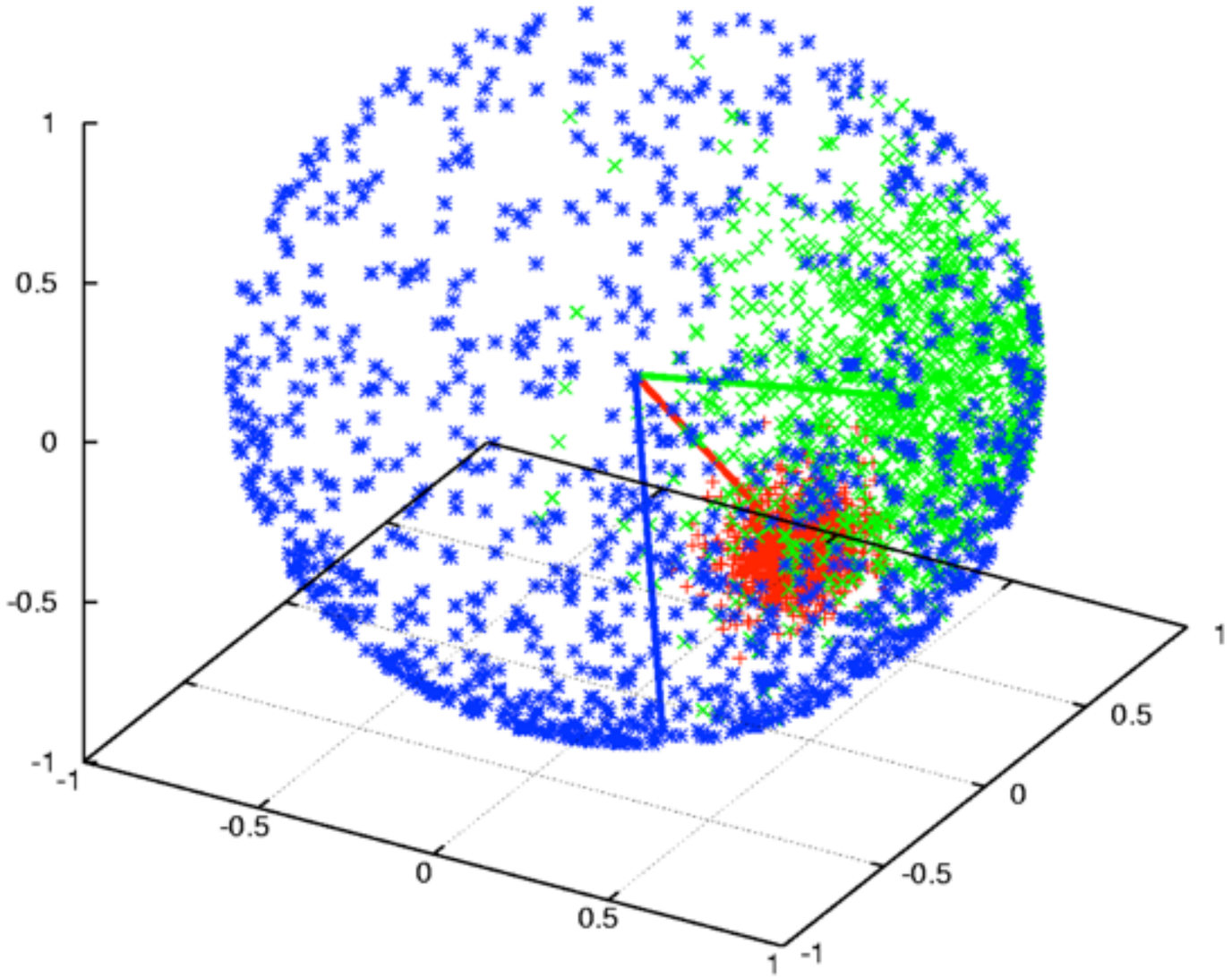

$\kappa = 1$

$\kappa = 10$

$\kappa = 100$

arrows = mean direction

dunkel@math.mit.edu

2.1.1 von Mises-Fisher (vMF) distribution

$$f(\boldsymbol{n}|\boldsymbol{\mu}) = C_2 e^{\kappa \boldsymbol{n}\cdot\boldsymbol{\mu}}. \tag{2.1}$$

$$\mathbb{E}[\boldsymbol{n}|\boldsymbol{\mu}] \;=\; C_2 \int dn\, \boldsymbol{n}\, e^{\kappa \boldsymbol{n}\cdot\boldsymbol{\mu}} = \left(\frac{1}{\tanh\kappa} - \frac{1}{\kappa}\right)\boldsymbol{\mu} =: \sigma\boldsymbol{\mu}, \tag{2.4a}$$

where the scale-factor $\sigma(\kappa)$ exhibits the following limiting behaviors

$$\lim_{\kappa\to 0}\sigma(\kappa) \;=\; 0, \tag{2.4b}$$

$$\lim_{\kappa\to\infty}\sigma(\kappa) \;=\; 1. \tag{2.4c}$$

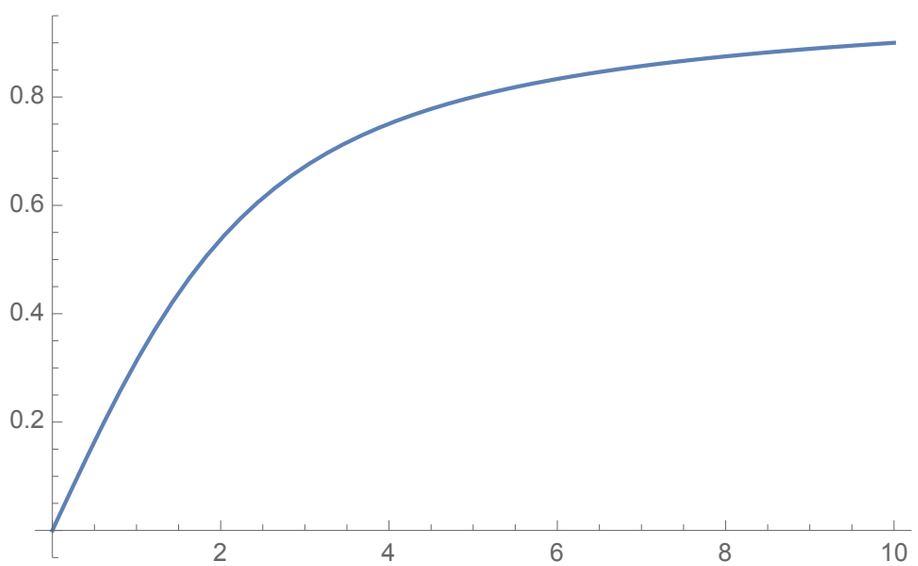

dunkel@math.mit.edu

2.1.2 vMF polymer model

Consider an idealized polymer consisting of $i = 1, \dots, N$ segments of length λ. Each segment has an orientation $\boldsymbol{\mu}_i$, so that the vector connecting the two polymer ends is given by

$$\boldsymbol{R}(N) = \sum_{i=1}^{N} \boldsymbol{R}_i = \lambda \sum_{i=1}^{N} \boldsymbol{\mu}_i. \tag{2.5}$$

The total length of the polymer is $L = N\lambda$ and w.l.o.g. we choose $\boldsymbol{R}(0)$ and $\boldsymbol{\mu}_1 = (0, 0, 1)$. We assume that the conditional PDF of $\boldsymbol{\mu}_i$ for a given $\boldsymbol{\mu}_{i-1}$, is a vMF-distribution with spread parameter κ,

$$f(\boldsymbol{\mu}_i | \boldsymbol{\mu}_{i-1}) = C_2 e^{\kappa \boldsymbol{\mu}_i \cdot \boldsymbol{\mu}_{i-1}}. \tag{2.6}$$

Karjalainen et al (2014) Polym Chem

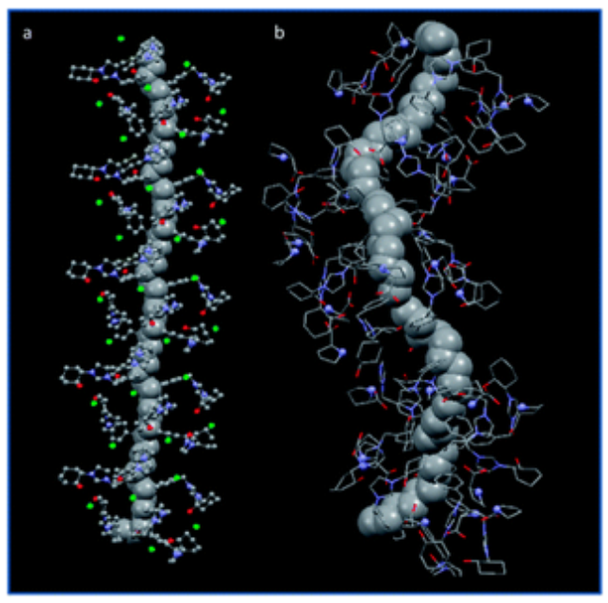

http://dx.doi.org/10.1039/1759-9962/2010

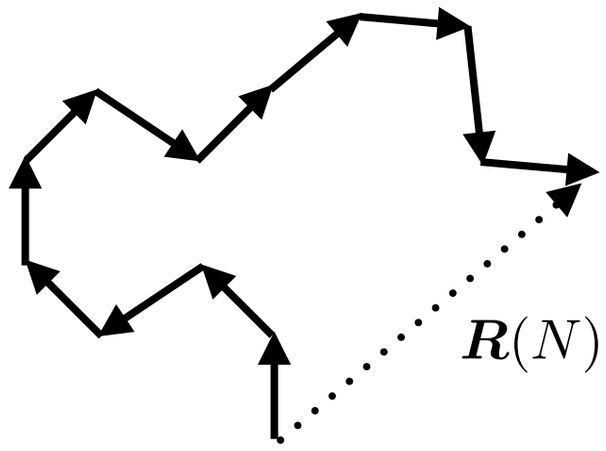

dunkel@math.mit.edu

$$\boldsymbol{R}(N) = \sum_{i=1}^{N} \boldsymbol{R}_i = \lambda \sum_{i=1}^{N} \boldsymbol{\mu}_i.$$

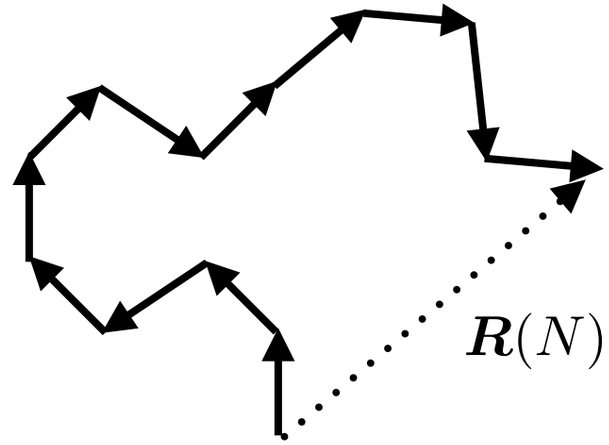

We would like to compute correlation functions and statistical moments of $\boldsymbol{R}(N)$ in the limit of large N. Of particular interest are the mean end-position

$$\mathbb{E}[\boldsymbol{R}(N)|\boldsymbol{\mu}_1] = \lambda \sum_{n=1}^{N} \mathbb{E}[\boldsymbol{\mu}_n|\boldsymbol{\mu}_1], \tag{2.7a}$$

the squared end-to-end distance

$$\mathcal{D}(N) = \mathbb{E}[\boldsymbol{R}(N) \cdot \boldsymbol{R}(N)], \tag{2.7b}$$

and the excursion PDF

$$p_N(\boldsymbol{r}) = \mathbb{E}\big[\delta(\boldsymbol{r} - \boldsymbol{R}(N))\big]. \tag{2.7c}$$

dunkel@math.mit.edu

$$\mathbb{E}[\boldsymbol{R}(N)|\boldsymbol{\mu}_1] = \lambda \sum_{n=1}^{N} \mathbb{E}[\boldsymbol{\mu}_n|\boldsymbol{\mu}_1],$$

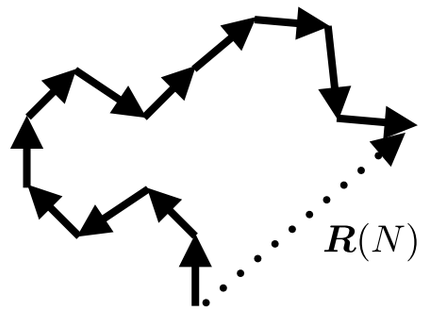

Mean end-position and persistence length

To compute the mean end-position $\mathbb{E}[\boldsymbol{R}(N)|\boldsymbol{\mu}_1]$ for a given initial condition $\boldsymbol{\mu}_1$, let us first note that the conditional expectation value $\mathbb{E}[\boldsymbol{\mu}_n|\boldsymbol{\mu}_1]$ can be computed as

$$\begin{aligned}
\mathbb{E}[\boldsymbol{\mu}_n|\boldsymbol{\mu}_1] &= C_2^{n-1} \int \boldsymbol{\mu}_n \, e^{\kappa \sum_{i=2}^{N} \boldsymbol{\mu}_i \cdot \boldsymbol{\mu}_{i-1}} \prod_{i=2}^{n} d\mu_i \\
&= \sigma \, C_2^{n-2} \int \boldsymbol{\mu}_{n-1} \, e^{\kappa \sum_{i=2}^{n-1} \boldsymbol{\mu}_i \cdot \boldsymbol{\mu}_{i-1}} \prod_{i=2}^{n-1} d\mu_i \\
&\cdots \\
&= \sigma^{n-1} \boldsymbol{\mu}_1, \qquad (2.8)
\end{aligned}$$

dunkel@math.mit.edu

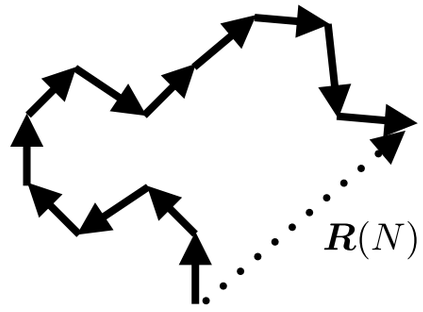

Mean end-position and persistence length

$$\mathbb{E}[\boldsymbol{R}(N)|\boldsymbol{\mu}_1] \;=\; \lambda\sum_{n=1}^{N}\sigma^{n-1}\,\boldsymbol{\mu}_1 = \lambda\sum_{n=0}^{N-1}\sigma^{n}\,\boldsymbol{\mu}_1 = \lambda\frac{1-\sigma^N}{1-\sigma}\,\boldsymbol{\mu}_1$$

In the limit case of a uniform distribution, $\kappa \to 0$, we find at fixed N

$$\mathbb{E}[\boldsymbol{R}(N)|\boldsymbol{\mu}_1] = \lambda\boldsymbol{\mu}_1 \tag{2.10a}$$

whereas for an infinitely stiff polymer with $\kappa \to \infty$

$$\mathbb{E}[\boldsymbol{R}(N)|\boldsymbol{\mu}_1] = \lambda N\boldsymbol{\mu}_1, \tag{2.10b}$$

illustrating that the vMF-model interpolates between undirected random walking and ballistic motion.

dunkel@math.mit.edu

Mean end-position and persistence length L_P

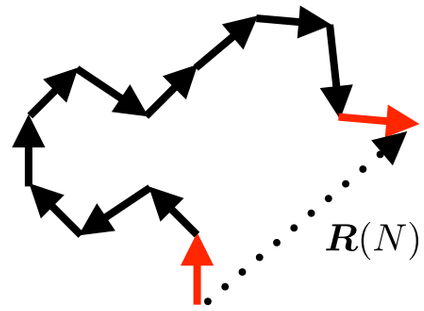

$$\langle \cos \theta_N \rangle \equiv \mathbb{E}[\boldsymbol{\mu}_N \cdot \boldsymbol{\mu}_1] \simeq e^{-L/L_P} \tag{2.11}$$

for large polymer length $L = N\lambda$. Noting that

$$\mathbb{E}[\boldsymbol{\mu}_N \cdot \boldsymbol{\mu}_1] = \mathbb{E}[\boldsymbol{\mu}_N | \boldsymbol{\mu}_1] \cdot \boldsymbol{\mu}_1, \tag{2.12}$$

dunkel@math.mit.edu

Mean end-position and persistence length L_P

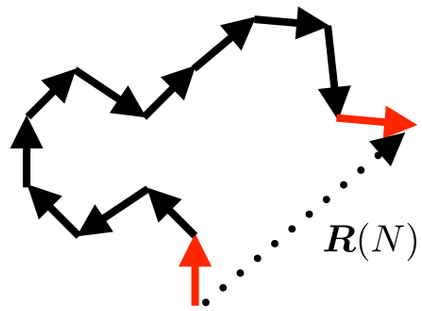

$$\langle \cos\theta_N \rangle \equiv \mathbb{E}[\boldsymbol{\mu}_N \cdot \boldsymbol{\mu}_1] \simeq e^{-L/L_P} \tag{2.11}$$

for large polymer length $L = N\lambda$. Noting that

$$\mathbb{E}[\boldsymbol{\mu}_N \cdot \boldsymbol{\mu}_1] = \mathbb{E}[\boldsymbol{\mu}_N|\boldsymbol{\mu}_1] \cdot \boldsymbol{\mu}_1, \tag{2.12}$$

we can obtain L_P from (2.8) by

$$\begin{aligned} \frac{1}{L_P} &= -\lim_{L\to\infty} \frac{1}{L} \ln \mathbb{E}[\boldsymbol{\mu}_N \cdot \boldsymbol{\mu}_1] \\ &= -\lim_{N\to\infty} \frac{1}{\lambda N} \ln \sigma^{N-1} \\ &= -\frac{1}{\lambda} \ln \sigma. \end{aligned} \tag{2.13}$$

dunkel@math.mit.edu

Mean end-position and persistence length L_P

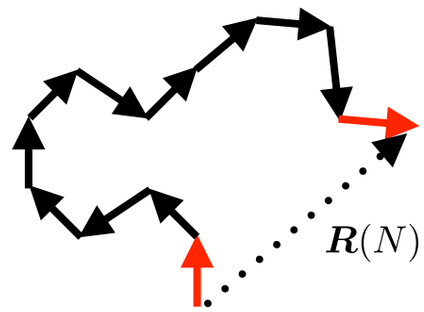

$$\langle \cos\theta_N \rangle \equiv \mathbb{E}[\boldsymbol{\mu}_N \cdot \boldsymbol{\mu}_1] \simeq e^{-L/L_P} \tag{2.11}$$

for large polymer length $L = N\lambda$. Noting that

$$\mathbb{E}[\boldsymbol{\mu}_N \cdot \boldsymbol{\mu}_1] = \mathbb{E}[\boldsymbol{\mu}_N|\boldsymbol{\mu}_1] \cdot \boldsymbol{\mu}_1, \tag{2.12}$$

we can obtain L_P from (2.8) by

$$\begin{aligned} \frac{1}{L_P} &= -\lim_{L\to\infty} \frac{1}{L} \ln \mathbb{E}[\boldsymbol{\mu}_N \cdot \boldsymbol{\mu}_1] \\ &= -\lim_{N\to\infty} \frac{1}{\lambda N} \ln \sigma^{N-1} \\ &= -\frac{1}{\lambda} \ln \sigma. \end{aligned} \tag{2.13}$$

Inserting the explicit expression $\sigma(\kappa)$ from (2.4a), we find for $\kappa \ll 1$

$$L_P \simeq \frac{\lambda}{\ln(3/\kappa)}, \tag{2.14a}$$

whereas for $\kappa \gg 1$

$$L_P \simeq \lambda\kappa. \tag{2.14b}$$

dunkel@math.mit.edu

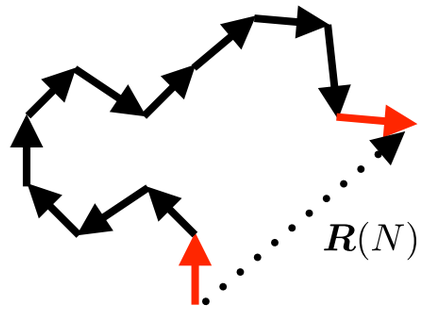

Squared end-to-end distance

To compute the squared end-to-end distance

$$\mathcal{D}(N) \quad = \quad \mathbb{E}[\boldsymbol{R}(N)\cdot\boldsymbol{R}(N)] = \lambda^2 \sum_{i,j=1}^{N} \mathbb{E}[\boldsymbol{\mu}_i \cdot \boldsymbol{\mu}_j], \tag{2.15}$$

we may use that the orientation correlation is translation-invariant

$$\mathbb{E}[\boldsymbol{\mu}_i \cdot \boldsymbol{\mu}_j] = \sigma^{|i-j|}. \tag{2.16}$$

Computing the double sum (2.15), one obtains

$$\mathcal{D}(N) = \lambda^2 \frac{N - \sigma\left(2 - 2\sigma^N + \sigma N\right)}{(\sigma-1)^2}, \tag{2.17}$$

and from this the limiting behaviors

$$\lim_{\kappa\to 0} \mathcal{D}(N) \quad = \quad \lim_{\sigma\to 0} \mathcal{D}(N) = \lambda^2 N, \tag{2.18a}$$

$$\lim_{\kappa\to \infty} \mathcal{D}(N) \quad = \quad \lim_{\sigma\to 1} \mathcal{D}(N) = \lambda^2 N^2, \tag{2.18b}$$

corresponding to normal diffusion and ballistic growth. Conversely, when keeping $\kappa < \infty$ fixed but letting the number of monomers $N \to \infty$, then

$$D(\kappa) := \lim_{N\to\infty} \frac{\mathcal{D}}{N} = \lambda^2 \frac{1+\sigma}{1-\sigma}, \tag{2.18c}$$

dunkel@math.mit.edu

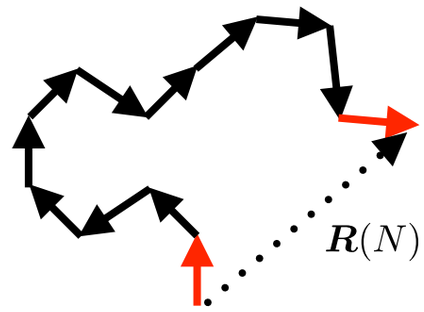

Squared end-to-end distance

To compute the squared end-to-end distance

$$\mathcal{D}(N) \;=\; \mathbb{E}[\boldsymbol{R}(N)\cdot\boldsymbol{R}(N)] = \lambda^2\sum_{i,j=1}^{N}\mathbb{E}[\boldsymbol{\mu}_i\cdot\boldsymbol{\mu}_j], \tag{2.15}$$

$$\lim_{\kappa\to 0}\mathcal{D}(N) \;=\; \lim_{\sigma\to 0}\mathcal{D}(N) = \lambda^2 N, \tag{2.18a}$$

$$\lim_{\kappa\to \infty}\mathcal{D}(N) \;=\; \lim_{\sigma\to 1}\mathcal{D}(N) = \lambda^2 N^2, \tag{2.18b}$$

corresponding to normal diffusion and ballistic growth. Conversely, when keeping $\kappa<\infty$ fixed but letting the number of monomers $N\to\infty$, then

$$D(\kappa) := \lim_{N\to\infty}\frac{\mathcal{D}}{N} = \lambda^2\frac{1+\sigma}{1-\sigma}, \tag{2.18c}$$

This means that, for finite κ, the end-to-end distance increases with $N^{1/2}$ corresponding to normal diffusion. For floppy polymers with $\kappa\to 0$, one finds that $D\to\lambda^2$, whereas for large κ

$$\lim_{\kappa\to\infty}\frac{D}{\kappa} = 2\lambda^2. \tag{2.19}$$

That is, for long stiff polymers with $\kappa\gg 1$, we have

$$D\simeq 2\lambda^2\kappa = 2\lambda L_P. \tag{2.20}$$

dunkel@math.mit.edu

Excursion PDF & thermodynamics

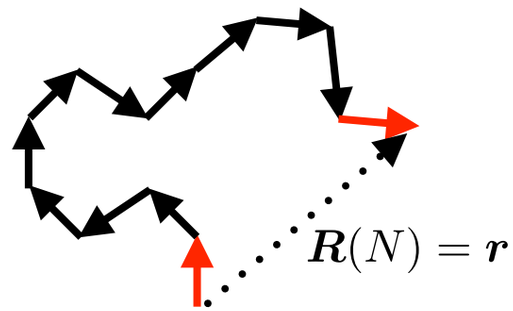

$$p_N(\boldsymbol{r}) = \mathbb{E}\big[\delta(\boldsymbol{r} - \boldsymbol{R}(N))\big]$$

Unfortunately, it is not possible to compute the excursion PDF (2.7c) exactly for the vMF model[1]. However, the central limit theorem combined with (2.18c) implies that, for large N, the excursion PDF will approach a Gaussian

$$p(\boldsymbol{r}) \simeq \left(\frac{3}{2\pi DN}\right)^{3/2} e^{-3\boldsymbol{r}^2/(2DN)}. \tag{2.21}$$

For the remainder of this section, we will assume that the end-points of the polymer are fixed at $\mathbf{0}$ and $\boldsymbol{r}$. To make the connection with thermodynamics, we may consider $\boldsymbol{r}$ as a *macroscopic* state-variable, that can be realized by a number of different polymer configurations referred to as *microstates*. If no other constraints are known, it is plausible that each microstate is equally likely and, for large N, the number of microstates realizing a specific the macrostate $\boldsymbol{r}$ is $\lambda^3 p(\boldsymbol{r})$, assuming the spatial resolution is of the order of the segment length λ. The corresponding microcanonical entropy is given by

$$S \simeq k_B \ln[\lambda^3 p(\boldsymbol{r})] = S_0 - k_B \frac{3\boldsymbol{r}^2}{2DN}. \tag{2.22}$$

dunkel@math.mit.edu

Excursion PDF & thermodynamics

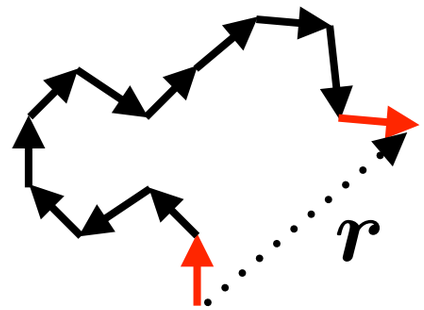

$$S \simeq k_B \ln[\lambda^3 p(\boldsymbol{r})] = S_0 - k_B \frac{3\boldsymbol{r}^2}{2DN}$$

To obtain a prediction for the mean force $\boldsymbol{f}$ required to stretch the polymer by a small amount $d\boldsymbol{r}$, we can exploit the general thermodynamic relation

$$dE = \delta W + \delta Q, \tag{2.23a}$$

where work and heat increments are defined as usual by

$$\delta W = -\boldsymbol{f} \cdot d\boldsymbol{r}\ , \qquad \delta Q = T dS, \tag{2.23b}$$

with T denoting temperature. If one neglect self-avoidance interactions, which are present in real polymers, the energy remains constant during a change of confirmation, $dE = 0$. Hence,

$$dS = \frac{\boldsymbol{f}}{T} \cdot d\boldsymbol{r} \tag{2.24}$$

and the stretch force components are obtained as

$$f_i = T\left(\frac{\partial S}{\partial r_i}\right) = -\frac{3k_B T}{DN} r_i. \tag{2.25}$$

$-\boldsymbol{f}$ is the force needed to stretch a polymer in a solvent bath of temperature T

Excursion PDF & thermodynamics

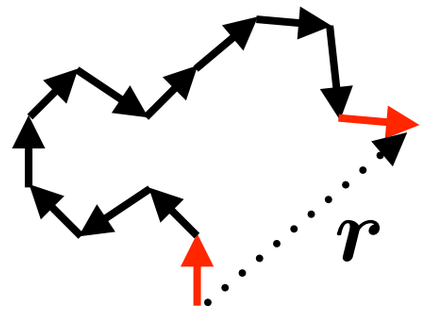

$$S \simeq k_B \ln[\lambda^3 p(\boldsymbol{r})] = S_0 - k_B \frac{3\boldsymbol{r}^2}{2DN}$$

Furthermore, it is also instructive to compute the corresponding free-energy

$$F := E - TS = E - TS_0 + k_B T \, \frac{3\boldsymbol{r}^2}{2DN}. \tag{2.26}$$

This is essentially a thermodynamic version of Hooke's law

$$F = F_0 + \frac{K}{2}\boldsymbol{r}^2 \, , \qquad K = \frac{3k_B T}{DN}. \tag{2.27}$$

For long stiff polymers we have $DN \simeq 2\lambda N L_P = 2LL_P$, we find for the spring-constant

$$K = \frac{3k_B T}{2LL_P}. \tag{2.28}$$

This means, for example, that the persistence length L_p can be inferred from force measurements if temperature T and polymer length L are known.

dunkel@math.mit.edu

Self-avoidance (Flory's scaling argument)

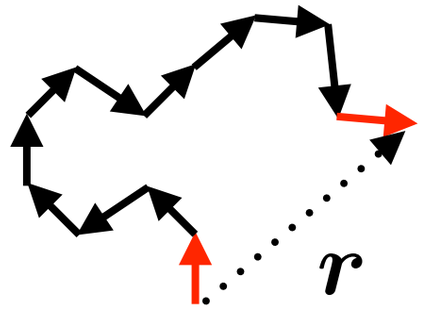

$$F = F_0 + \frac{K}{2}\boldsymbol{r}^2 \,, \qquad K = \frac{3k_BT}{DN}$$

- IDEA: include additional free energy term to account for self repulsion

- ASSUMPTIONS:

(i) $N \gg 1$ monomers of volume v_d with fixed end-to-end distance $\boldsymbol{r}$

(ii) for a fixed $|\boldsymbol{r}|$, the N monomers may (very roughly) explore a volume of $|\boldsymbol{r}|^d$,

(iii) overlap probability given by volume filling fraction $\phi = v_d N/|\boldsymbol{r}|^d$

$$F_e \simeq Nk_BT\,\phi = Nk_BT\,\frac{v_dN}{|\boldsymbol{r}|^d} \qquad \Rightarrow \qquad F = F_0 + Nk_BT\left(\frac{v_dN}{|\boldsymbol{r}|^d} + \frac{|\boldsymbol{r}|^2 d}{2D_dN^2}\right)$$

dunkel@math.mit.edu

Self-avoidance (Flory's scaling argument)

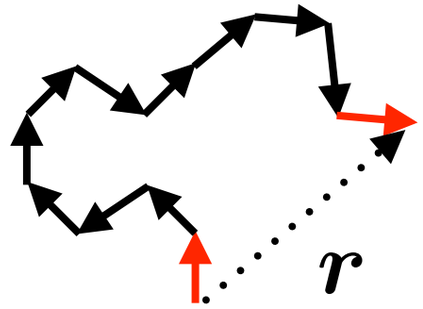

$$F = F_0 + Nk_BT\left(\frac{v_dN}{|\boldsymbol{r}|^d} + \frac{|\boldsymbol{r}|^2 d}{2D_dN^2}\right). \tag{2.30}$$

To obtain the equilibrium distance r_*, we must minimize this expression with respect to $r = |\boldsymbol{r}|$, which gives

$$0 = \frac{dF}{d|\boldsymbol{r}|} = -d\frac{v_dN}{r_*^{d+1}} + \frac{d}{D_dN^2}r_* \tag{2.31}$$

and therefore

$$r_* = (D_dv_d)^{1/d+2}N^{3/(d+2)}. \tag{2.32}$$

Thus, explicitly

$$d = 1: \qquad r_* \propto N \tag{2.33a}$$
$$d = 2: \qquad r_* \propto N^{3/4}, \tag{2.33b}$$
$$d = 3: \qquad r_* \propto N^{3/5}. \tag{2.33c}$$

The result is trivial for $d = 1$, seems to be exact for $d = 2$ when compared to simulations, and is very close to best numerical results $N^{0.589\ldots}$ for $d = 3$.

dunkel@math.mit.edu

Rouse model (wiki)

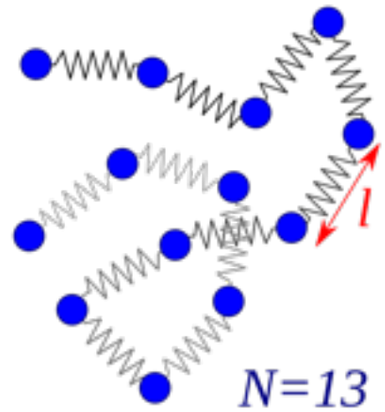

2.2 Bead-spring model

single bead is governed by the over-damped Langevin equation

$$d\boldsymbol{X}_\alpha(t) = -\nabla_{\boldsymbol{x}_\alpha} U(\{\boldsymbol{X}_\alpha\})\, dt + \sqrt{2D} * d\boldsymbol{B}_\alpha(t), \tag{2.34}$$

where D is the thermal diffusion constant of a bead. The potential U contains contributions from elastic nearest neighbor interactions U_e, from bending U_b and, to implement self-avoidance, steric short-range repulsion U:

$$U = U_e + U_b + U_s \tag{2.35}$$

Defining $(N-1)$ chain link vectors $\boldsymbol{R}_\alpha$ and their orientations $\boldsymbol{\mu}_\alpha$ by

$$\boldsymbol{R}_\alpha = \boldsymbol{X}_{\alpha+1} - \boldsymbol{X}_\alpha\ , \qquad \boldsymbol{\mu}_\alpha = \frac{\boldsymbol{R}_\alpha}{||\boldsymbol{R}_\alpha||} \tag{2.36}$$

the potentials can be written as sums over 2-body and 3-body interactions

$$U_e = \sum_{\alpha=1}^{N-1} u(||\boldsymbol{R}_\alpha||). \qquad U_b = \sum_{\alpha=1}^{N-2} b(\boldsymbol{\mu}_\alpha \cdot \boldsymbol{\mu}_{\alpha+1}); \qquad U_s = \sum_{\alpha=1}^{N} \sum_{\beta=1,\beta\neq\alpha}^{N} s(||\boldsymbol{X}_\alpha - \boldsymbol{X}_\beta||).$$

Specifically, the elastic spring potential $u(r)$ and the steric repulsion potential $s(r)$ encode 2-body interactions, whereas the bending potential $b(q)$ involves 3-body interactions.[2] Plausible choices are

$$u(r) = \frac{K}{2}(r-\lambda)^2\ , \qquad b(q) = \frac{B}{2}(q-1)^2\ , \qquad s(r) = \frac{S\, e^{-r/\sigma}}{r^\nu} \tag{2.38}$$

dunkel@math.mit.edu

Rouse model (wiki)

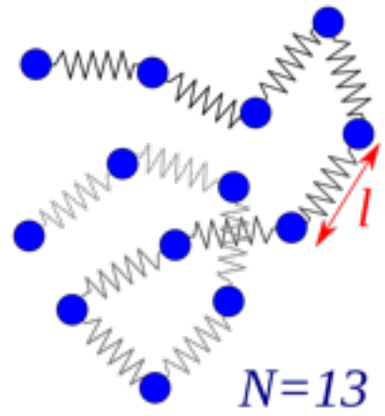

2.2 Bead-spring model

single bead is governed by the over-damped Langevin equation

$$d\boldsymbol{X}_\alpha(t) = -\nabla_{\boldsymbol{x}_\alpha} U(\{\boldsymbol{X}_\alpha\})\, dt + \sqrt{2D} * d\boldsymbol{B}_\alpha(t), \tag{2.34}$$

where D is the thermal diffusion constant of a bead. The potential U contains contributions from elastic nearest neighbor interactions U_e, from bending U_b and, to implement self-avoidance, steric short-range repulsion U:

$$U = U_e + U_b + U_s \tag{2.35}$$

Needs to be solved numerically but stationary distribution known

$$p_N(\{\boldsymbol{x}_\alpha\}) = \frac{1}{Z_N} \exp\left[-\frac{U(\{\boldsymbol{X}_\alpha\})}{D}\right], \tag{2.39}$$

where

$$Z_N = \int \left(\prod_{\alpha=1}^{N} d^3 x_\alpha\right) \exp\left[-\frac{U(\{\boldsymbol{x}_\alpha\})}{D}\right]. \tag{2.40}$$

dunkel@math.mit.edu